# A STRUCTURE PRESERVING ENERGY FUNCTION FOR POWER SYSTEM TRANSIENT STABILITY ANALYSIS

by

N. Tsolas, A. Arapostathis and P. Varaiya

Memorandum No. UCB/ERL M84/1

3 January 1984

ELECTRONICS RESEARCH LABORATORY

College of Engineering
University of California, Berkeley
94720

# A STRUCTURE PRESERVING ENERGY FUNCTION FOR POWER SYSTEM TRANSIENT STABILITY ANALYSIS[1]

*N. Tsolas*[2], *A. Arapostathis*[3] *and P. Varaiya*

Department of Electrical Engineering and Computer Sciences
and Electronics Research Laboratory
University of California, Berkeley CA 94720

*ABSTRACT*

A new model is proposed for the study of transient stability where the load is modeled as a PQ bus. Flux decay of the generator field winding is included. The original network topology is maintained explicitly. An energy function is proposed which differs from the traditional one in that it includes additional terms corresponding to the energy stored in the loads and field winding. The new energy function eliminates the difficulties in earlier approaches arising from transfer conductances. Moreover, the preservation of the network topology in the energy function makes it much more suitable for on-line security assessment.

January 3, 1984

# A STRUCTURE PRESERVING ENERGY FUNCTION FOR POWER SYSTEM TRANSIENT STABILITY ANALYSIS[1]

*N. Tsolas*[2], *A. Arapostathis*[3] *and P. Varaiya*

Department of Electrical Engineering and Computer Sciences
and Electronics Research Laboratory
University of California, Berkeley CA 94720

## 1. Introduction

The use of energy functions in power system transient analysis is now well established. These functions are used to estimate the domain of attraction of a stable equilibrium point. The standard approach to constructing energy functions is facilitated by three modeling choices: a generator is modeled by the classical swing equation, a load is taken to be a constant impedance, and the entire network is reduced to an n-port as seen from the n generator internal buses.

These choices impose several limitations. The classical swing equation assumes a constant field flux linkage which is unrealistic. While it may be conceded that in the time period of interest one can reasonably ignore governor and exciter feedback effects, critics contend that flux decay cannot be ignored. In the model used here, the classical model is augmented by a flux decay relation to yield what Anderson and Fouad [1] call the "one-axis" model. From the vantage point of this augmented model it will be seen that the classical equations generally give more conservative estimates of the region of stability.

[1]Research supported by DOE contracts DE-AS01-78ET29135 and DE-AC01-82-CE76221 and NSF grants ECS-7903879 and ECS-8118213. The authors are grateful to Prof. Felix Wu, Eyad Abed, Fathi Abdel-Salam, Kemal Inan and R-L. Chen for many helpful discussions.
[2]Present address: Bell Laboratories, Holmdel NJ 07733
[3]Present address: Dept. of Electrical Engineering, University of Texas, Austin TX 78712

Second, in this study the load the load bus is viewed as a constant PQ bus. This is generally accepted as being more realistic. It also conforms with the practice in load flow studies.

Third, the reduction of the network to an n-port entails two deficiencies. On the one hand, this introduces transfer conductances even when the transmission lines are lossless. To obtain an energy function one is then led to ignore these transfer conductances creating an error of unknown magnitude. Alternatively, if one chooses not to ignore the transfer conductances, then one is faced with the computationally cumbersome and mathematically unsound practice of defining the energy function via path-dependant integrals. In contrast, the energy function proposed here is exact for PQ loads and lossless lines.

Reduction of the network to an n-port erases the network topology making it impossible to allocate the aggregate energy to the components of the network. As a result, changes in energy during a transient cannot be decomposed into energy shifts occurring in individual power system elements. Since the proposed energy function is the sum of the energy of each individual component, as will be seen in the illustrative examples given below, this provides an insightful description of the transfer of energy during the transient. One other attempt to provide a "structure preserving" Lyapunov function [8] is limited by the requirement that loads be modeled as PV buses.

Finally, the proposed energy function is expressed in two forms. The first is more useful for purposes of mathematical analysis. The second is especially appealing from the viewpoint of computation and practical implementation since the expression involves only terminal measurements.

This paper is structured as follows. The one-axis model, as well as the classical model, are presented in Section 2. The energy function is derived in Section 3, and alternative forms are given in Section 4. Key stability results occupy

Section 5, whereas Section 6 is devoted to the evaluation of the critical clearing time. Examples may be found in Section 7. All the figures are collected at the end of the paper.

## 2. Model

### 2.1. The network

The power network consists of n+m+1 nodes or buses connected by lossless transmission lines. It is represented by its node admittance matrix $Y = [Y_{ij}]$, where $Y_{ij} = -jB_{ij}$, and $B_{ij}$ is the susceptance of the line connecting buses i and j. The first n nodes are the terminal buses of the generators. Bus n+1 is an infinite bus. These buses are indexed by i or j = 1,2,...,n+1. Each terminal generator bus is connected with its internal generator bus through a lossless line (armature resistance of the stator is neglected) with reactance equal to $x'_d$, the generator transient reactance. The remaining m nodes are the load buses. These are indexed by k or l = n+2,.....,n+m+1. Let $E_i \angle \delta_i$ denote the internal voltage phasor and $V_i \angle \vartheta_i$ denote the terminal voltage phasor of the $i^{th}$ generator. Let $V_k \angle \varphi_k$ denote the voltage phasor of the $k^{th}$ load bus. All phase angles are measured relative to the infinite bus i.e. $\vartheta_{n+1} \equiv 0$. Furthermore $V_{n+1} = 1$. p.u..

### 2.2. Loads

Each load is represented as a constant real ($P^d$) and reactive ($Q^d$) power demand. Therefore we refer to a load bus as a PQ bus.

## 2.3. Generator Model

It is generally agreed that in transient stability studies, generators close to the fault should be modeled in greater detail. The complexity of a generator model depends on how many of the rotor windings have been represented. Two models are considered here.

### 2.3.1. The One-axis Model

This model includes one circuit for the field winding of the rotor. For a complete description and more details see [1,37]. The model is given by the following differential and algebraic equations.

For generator i

$$\dot{\delta}_i = 2\pi f(\omega_i - 1) \tag{2.1}$$

$$M_i \dot{\omega}_i = P_i^m - D_i(\omega_i - 1) - E'_{q_i} I_{q_i} + (x_{q_i} - x'_{d_i}) I_{q_i} I_{d_i} \tag{2.2}$$

$$T'_{do_i} \dot{E}'_{q_i} = -E'_{q_i} + (x_{d_i} - x'_{d_i}) I_{d_i} + E_{F_i} \tag{2.3}$$

$$V_{q_i} = E'_{q_i} + x'_{d_i} I_{d_i} \tag{2.4}$$

$$V_{d_i} = -x_{q_i} I_{d_i} \tag{2.5}$$

$$V_i e^{j\theta_i} = (V_{q_i} + jV_{d_i}) e^{j\delta_i} \tag{2.6}$$

where,

$f$ = Synchronous frequency (60 Hz)

$P_i^m$ = Mechanical power (torque)

$M_i$ , $D_i$ = Moment of inertia and damping coefficient

$x_{d_i}$ , $x_{q_i}$ = Direct and quadrature axis synchronous reactance

$x'_{d_i}$ = Direct axis transient reactance ( $x'_{d_i} < x_{d_i}, x_{q_i}$ )

$T'_{do_i}$ = Direct axis transient open-circuit time constant

$E'_{q_i}$ = Quadrature axis voltage behind transient reactance

$E_{F_i}$ = Voltage behind synchronous reactance

$V_{q_i}, V_{d_i}, I_{q_i}, I_{d_i}$ = Quadrature and direct axis components of terminal voltage and current.

The mechanical power $P_i^m$ is assumed constant. $E_{F_i}$ is the output of the exciter and is also constant. The internal generator voltage is $E'_i$ with $E'_{q_i}$ its component along the quadrature axis. Figure 1 shows the phasor diagram of the stator.

The field winding is modeled as a linear RLC circuit. The flux linkage, $\Phi_{F_i}$, is given by

$$\Phi_{F_i} = L_{F_i} I_{F_i} + L_{AD_i} I_{d_i} \tag{2.7}$$

where $L_{F_i}, L_{AD_i}$ is the self and mutual inductance respectively. Equation (2.3) can also be written as

$$\Phi_{F_i} = -r_{F_i} I_{d_i} + V_{F_i} \tag{2.8}$$

where $r_{F_i}$ is the field resistance and $V_{F_i}$ is the field voltage. Finally[4]

$$E'_{q_i} = \frac{L_{AD_i}}{L_{F_i}} \Phi_{F_i} \tag{2.9}$$

### 2.3.2. The Classical Model

If we assume that $\Phi_{F_i}$ is constant, or equivalently $E'_{q_i}$ is constant, and $x_{q_i} = x'_{d_i}$ then we have the so called "classical" model. It assumes a constant voltage behind a transient reactance and it has been used widely in transient stability studies. The motion of generator i is governed by the "swing" equation,

$$\dot{\delta}_i = 2\pi f(\omega_i - 1) \tag{2.10}$$

$$M_i \dot{\omega}_i = P_i^m - D_i(\omega_i - 1) - \frac{E_i V_i \sin(\delta_i - \vartheta_i)}{x'_{d_i}} \tag{2.11}$$

where $E'_{q_i}$ has been replaced by $E_i$, the internal generator voltage.

In both models the effects of the amortisseur or damper windings have been neglected as being very small during a transient. As suggested in [1], in some cases, these effects may be included in the damping torque i.e. by increasing the damping coefficient D.

## 3. Energy Functions

The terminal buses of the generators are modeled as PQ load buses with P = 0 and Q = 0. This means simply that they are treated as power distribution stations with no local loads.

[4] Depending on the choice of per unit base quantities a factor of $\sqrt{3}$ might be needed i.e. $\sqrt{3}E'_{q_i} = \cdots$

### 3.1. The One-axis Model

For a power system where the generators are represented by the one-axis model, the system equations are given by

$$\dot{\delta}_i = 2\pi f(\omega_i - 1) \tag{3.1}$$

$$M_i \dot{\omega}_i = P_i^m - D_i(\omega_i - 1) - P_i^e \tag{3.2}$$

$$\frac{T'_{do_i}}{x_{d_i} - x'_{d_i}} \dot{E}'_{q_i} = K_i(\delta, E'_q, \vartheta, V, \varphi) \tag{3.3}$$

$$i = 1,\ldots,n$$

where,

$$P_i^e = f_i(\delta, E'_q, \vartheta, V, \varphi) := \frac{V_i^2 \sin[2(\delta_i - \vartheta_i)](x'_{d_i} - x_{q_i})}{2 x_{q_i} x'_{d_i}} + \frac{E'_{q_i} V_i \sin(\delta_i - \vartheta_i)}{x'_{d_i}} \tag{3.4}$$

and

$$K_i(\delta, E'_q, \vartheta, V, \varphi) := -\frac{x_{d_i}}{x'_{d_i}(x_{d_i} - x'_{d_i})} E'_{q_i} + \frac{V_i \cos(\delta_i - \vartheta_i)}{x'_{d_i}} + \frac{1}{(x_{d_i} - x'_{d_i})} E_{F_i} \tag{3.5}$$

At the $i^{th}$ terminal generator bus, $i = 1,\ldots,n$, one gets

$$0 = g_i(\delta, E'_q, \vartheta, V, \varphi) := \frac{V_i^2 \sin[2(\vartheta_i - \delta_i)](x'_{d_i} - x_{q_i})}{2 x_{q_i} x'_{d_i}} +$$

$$\frac{E'_{q_i} V_i \sin(\vartheta_i - \delta_i)}{x'_{d_i}} + \sum_{j \neq i}^{n+1} B_{ij} V_i V_j \sin(\vartheta_i - \vartheta_j) +$$

$$\sum_{k=n+2}^{n+m+1} B_{ik} V_i V_k \sin(\vartheta_i - \varphi_k) \qquad (3.6)$$

$$0 = h_i(\delta, E'_q, \vartheta, V, \varphi) := \frac{x'_{d_i} + x_{q_i}}{2 x_{q_i} x'_{d_i}} V_i^2 - \frac{E'_{q_i} V_i \cos(\vartheta_i - \delta_i)}{x'_{d_i}} -$$

$$\frac{V_i^2 \cos[2(\vartheta_i - \delta_i)]\,(x'_{d_i} - x_{q_i})}{2 x_{q_i} x'_{d_i}} -$$

$$B_{ii} V_i^2 - \sum_{j \neq i}^{n+1} B_{ij} V_i V_j \cos(\vartheta_i - \vartheta_j) -$$

$$\sum_{k=n+2}^{n+m+1} B_{ik} V_i V_k \cos(\vartheta_i - \varphi_k) \qquad (3.7)$$

At the $k^{th}$ load bus, $k = n+2,\ldots,n+m+1$,

$$P_k^d = g_k(\delta, E'_q, \vartheta, V, \varphi) := \sum_{i=1}^{n+1} B_{ki} V_k V_i \sin(\varphi_k - \vartheta_i) +$$

$$\sum_{l \neq k}^{n+m+1} B_{kl} V_k V_l \sin(\varphi_k - \varphi_l) \qquad (3.8)$$

$$Q_k^d = h_k(\delta, E'_q, \vartheta, V, \varphi) := -B_{kk} V_k^2 - \sum_{i=1}^{n+1} B_{ki} V_k V_i \cos(\varphi_k - \vartheta_i) -$$

$$\sum_{l \neq k}^{n+m+1} B_{kl} V_k V_l \cos(\varphi_k - \varphi_l) \qquad (3.9)$$

Equations (3.1) - (3.9) constitute the system model. We can rewrite them in a more compact vector form

$$\dot{\delta} = 2\pi f(\omega - 1) \qquad (3.10)$$

$$M\dot{\omega} = P^m - D(\omega-1) - f(\delta, E'_q, \vartheta, V, \varphi) \tag{3.11}$$

$$\frac{T'_{do}}{x_d - x'_d} E'_q = K(\delta, E'_q, \vartheta, V, \varphi) \tag{3.12}$$

$$0 = P^d - g(\delta, E'_q, \vartheta, V, \varphi) \tag{3.13a}$$

$$0 = Q^d - h(\delta, E'_q, \vartheta, V, \varphi) \tag{3.13b}$$

Let $\Sigma_1$ denote the 2n-dimensional manifold or surface of all points $(\delta, E'_q, \vartheta, V, \varphi) \in R^{4n+2m}$ satisfying (3.13). Then the state for this model is $(\omega, \delta, E'_q, \vartheta, V, \varphi) \in R^n \times \Sigma_1$.

Obviously $V_i > 0$ , $i = 1,\ldots,n$. Assume that the load is never zero, that is, $(P_k^d)^2 + (Q_k^d)^2 > 0$. Then $V_k > 0$ , $k = n+2,\ldots,n+m+1$, and one may define new variables $\nu_i := \log V_i$ , $\nu_k = \log V_k$. Consider the function

$$V_1(\delta, E'_q, \vartheta, \nu, \varphi) := - \langle P^m, \delta \rangle - \langle P^d, \varphi \rangle - \langle Q^d, \nu \rangle - \left\langle \frac{E_F}{x_d - x'_d}, E'_q \right\rangle -$$

$$\sum_{i=1}^{n} \left[ B_{ii} + \frac{(x'_{d_i} - x_{q_i}) \cos[2(\delta_i - \vartheta_i)] - (x'_{d_i} - x_{q_i})}{2 x_{q_i} x'_{d_i}} \right] \frac{e^{2\nu_i}}{2} -$$

$$\sum_{i=1}^{n} \frac{E'_{q_i} e^{\nu_i} \cos(\delta_i - \vartheta_i)}{x'_{d_i}} + \sum_{i=1}^{n} \frac{x_{d_i}}{x'_{d_i}(x_{d_i} - x'_{d_i})} \frac{E'^2_{q_i}}{2} -$$

$$\sum_{i<j}^{n+1} B_{ij} e^{\nu_i + \nu_j} \cos(\vartheta_i - \vartheta_j) - \sum_{i=1}^{n+1} \sum_{k=n+2}^{n+m+1} B_{ik} e^{\nu_i + \nu_k} \cos(\vartheta_i - \varphi_k) -$$

$$\sum_{k<l}^{n+m+1} B_{kl} e^{\nu_k + \nu_l} \cos(\varphi_k - \varphi_l) - \sum_{k=n+2}^{n+m+1} B_{kk} \frac{e^{2\nu_k}}{2} \tag{3.14}$$

Let

$$W_1(\omega,\delta,E'_q,\vartheta,\nu,\varphi) := \frac{1}{2}(2\pi f)<(\omega-1),M(\omega-1)> +$$

$$V_1(\delta,E'_q,\vartheta,\nu,\varphi) \tag{3.15}$$

where $<...>$ denotes inner product.

Observe that

$$-\frac{\partial V_1}{\partial \delta_i} = P_i^m - f_i(\delta,E'_q,\vartheta,\nu,\varphi) \tag{3.16a}$$

$$-\frac{\partial V_1}{\partial E'_{q_i}} = K_i(\delta,E'_q,\vartheta,\nu,\varphi) \tag{3.16b}$$

$$-\frac{\partial V_1}{\partial \vartheta_i} = -g_i(\delta,E'_q,\vartheta,\nu,\varphi) \tag{3.16c}$$

$$-\frac{\partial V_1}{\partial \nu_i} = -h_i(\delta,E'_q,\vartheta,\nu,\varphi) \tag{3.16d}$$

$$-\frac{\partial V_1}{\partial \nu_k} = Q_k^d - h_k(\delta,E'_q,\vartheta,\nu,\varphi) \tag{3.16e}$$

$$-\frac{\partial V_1}{\partial \varphi_k} = P_k^d - g_k(\delta,E'_q,\vartheta,\nu,\varphi) \tag{3.16f}$$

$V_1$ is the potential and $W_1$ is the (total) energy function for this model. Using (3.16) it is easy to check that along the trajectories of the system we have

$$\frac{d}{dt}W_1(\omega,\delta,E'_q,\vartheta,\nu,\varphi) = -\sum_{i=1}^{n}[2\pi f D_i(\omega_i-1)^2 + \frac{T_{do_i}}{x_{d_i}-x'_{d_i}}E'^2_{q_i}] \le 0 \tag{3.17}$$

which shows that $W_1$ is a suitable Lyapunov function for the system. From [1,37] we have

$$T'_{do_i} = \frac{L_{F_i}}{r_{F_i}} \tag{3.18}$$

and

$$x_{d_i} - x'_{d_i} = \frac{L_{AD_i}^2}{L_{F_i}} \tag{3.19}$$

Using (3.18) , (3.19) and (2.9) we get

$$\frac{d}{dt} W_1(\omega, \delta, E'_q, \vartheta, \nu, \varphi) = -\sum_{i=1}^{n} [2\pi f D_i(\omega_i - 1)^2 + \frac{1}{r_{F_i}} \Phi_{F_i}^2] \leq 0 \tag{3.20}$$

which shows that the decrease in energy equals the dissipation due to damping and the power dissipated in the field winding.

### 3.2. The Classical Model

When the generators are represented by the classical model the system equations are given by

$$\dot{\delta} = 2\pi f(\omega - 1) \tag{3.21}$$

$$M\dot{\omega} = P^m - D(\omega - 1) - f(\delta, \vartheta, V, \varphi) \tag{3.22}$$

$$0 = P^d - g(\delta, \vartheta, V, \varphi) \tag{3.23a}$$

$$0 = Q^d - h(\delta, \vartheta, V, \varphi) \tag{3.23b}$$

where f, g, h can be easily obtained from (3.4) - (3.9) upon replacing $E'_{q_i}$ by $E_i$ and setting $x_{q_i} = x'_{d_i}$.

The state for this model is $(\omega, \delta, \vartheta, V, \varphi) \in R^n \times \Sigma_2$, where $\Sigma_2$ is the n-dimensional manifold or surface of all the points $(\delta, \vartheta, V, \varphi) \in R^{3n+2m}$ satisfying (3.23).

From (3.14) or from the model equations (3.21) - (3.23) we have

$$V_2(\delta,\vartheta,\nu,\varphi) := - <P^m,\delta> - <P^d,\varphi> - <Q^d,\nu> -$$

$$\sum_{i=1}^{n} \frac{E_i e^{\nu_i} \cos(\delta_i - \vartheta_i)}{x'_{d_i}} - \sum_{i=1}^{n} (B_{ii} - \frac{1}{x'_{d_i}}) \frac{e^{2\nu_i}}{2} -$$

$$\sum_{i<j}^{n+1} B_{ij} e^{\nu_i+\nu_j} \cos(\vartheta_i - \vartheta_j) - \sum_{i=1}^{n+1} \sum_{k=n+2}^{n+m+1} B_{ik} e^{\nu_i+\nu_k} \cos(\vartheta_i - \varphi_k) -$$

$$\sum_{k<l}^{n+m+1} B_{kl} e^{\nu_k+\nu_l} \cos(\varphi_k - \varphi_l) - \sum_{k=n+2}^{n+m+1} B_{kk} \frac{e^{2\nu_k}}{2} \qquad (3.24)$$

and

$$W_2(\omega,\delta,\vartheta,\nu,\varphi) := \frac{1}{2}(2\pi f) <(\omega-1), M(\omega-1)> + V_2(\delta,\vartheta,\nu,\varphi) \qquad (3.25)$$

Equations (3.16) are also satisfied for this model and

$$\frac{d}{dt} W_2(\omega,\delta,\vartheta,\nu,\varphi) = - \sum_{i=1}^{n} 2\pi f D_i (\omega_i - 1)^2 \leq 0 \qquad (3.26)$$

which was expected since $\Phi_{F_i}$, $i = 1,\ldots,n$, is constant for this model.

**Remark 3.1**

The inequalities (3.17) and (3.26) show that the energy functions can be used as Lyapunov functions. Moreover, the fact that (3.17) contains an additional dissipation term in comparison with (3.26) suggests that stability estimates based on the classical model will be more conservative than the estimates based on the

one-axis model.

**Remark 3.2**

These system models are to be interpreted as follows. One solves the algebraic equations (3.23) [ (3.13) ] for the unknowns $\vartheta, V, \varphi$ in terms of $\delta$ [$\delta$ and $E'_q$] and substitutes them into (3.21) - (3.22) [ (3.10) - (3.12) ] to obtain a system of differential equations in $\delta$ [$\delta$ and $E'_q$] alone. This procedure, however, yields a legitimate differential system in $\delta$ [$(\delta, E'_q)$] only if (3.23) [ (3.13) ] provides a solution $\vartheta, V, \varphi$ which is differentiable in $\delta$ [$\delta$ and $E'_q$]. From the Implicit Function Theorem, a sufficient condition for this is that the $2(n+m) \times 2(n+m)$ Jacobian matrix obtained by differentiating the function $(g\ ,\ h)$ with respect to $(\vartheta, V, \varphi)$ is nonsingular. While this nonsingularity may hold for reasonable values of $(\delta, \vartheta, V, \varphi)$ [$(\delta, E'_q, \vartheta, V, \varphi)$] in $\Sigma_2$ [$\Sigma_1$] it is easy to see that it cannot hold for all possible values. One way of overcoming this difficulty is to permit the trajectories to have a discontinuity or jump whenever the Jacobian becomes singular. This extension is defined via singular perturbations as in [23]. If in addition we assume that the energy function does not increase at these jumps then it is a global Lyapunov function. Alternatively, one may restrict the possible states to those initial values from which issue smooth trajectories over the infinite future. This alternative will be followed here. More precisely, let $S_2$ [$S_1$] be the set of all states $x = (\omega, \delta, \vartheta, V, \varphi)$ [$x = (\omega, \delta, E'_q, \vartheta, V, \varphi)$] in $R^n \times \Sigma_2$ [$R^n \times \Sigma_1$] such that for all $x \in S_2$ [$x \in S_1$] there is a differentiable function $x(t)$, $0 \le t < \infty$, with $x(0) = x$ and which satisfies (3.21) - (3.23) [ (3.10) - (3.13) ] for all t. Henceforth the system model is taken to be (3.21) - (3.23) [ (3.10) - (3.13) ] with the state space $S_2$ [$S_1$], and time derivatives of the energy function are taken along smooth trajectories.

**Remark 3.3**

Since $(\omega, \delta, \vartheta, V, \varphi)$ [$(\omega, \delta, E'_q, \vartheta, V, \varphi)$] is an equilibrium of (3.21) - (3.23) [

(3.10) - (3.13) ] iff $\omega = 1$ and $P^m - f(\delta, \vartheta, V, \varphi) = 0$ [ $\omega = 1$, $E'_q = 0$ and $P^m - f(\delta, E'_q, \vartheta, V, \varphi) = 0$ ] the point $(\delta, \vartheta, V, \varphi)$ [ $(\delta, E'_q, \vartheta, V, \varphi)$ ] will also be called an equilibrium.

## 4. Disaggregation and Reformulation

### 4.1. Disaggregation of the Total Energy

Consider the classical model. One of the main advantages of the proposed energy function is that the potential energy of an individual line or group of lines can be calculated explicitly. There are many ways to re-group the terms of (3.15) or (3.25). In [18] it is shown that the potential energy stored in a lossless transmission line is equal to half of the reactive power loss in that line. Motivated by this we have the following terms (separate indexing of the terminal generator buses from the loads is now very helpful).

$$V_{kin} := \frac{1}{2}(2\pi f)<(\omega-1), M(\omega-1)> \tag{4.1}$$

$$V_{P_m} := - <P_m, \delta> \tag{4.2}$$

$$V_{P_l} := - <P^d, \varphi> \tag{4.3}$$

$$V_{Q_l} := - <Q^d, \nu> = <Q^d, \log V> \tag{4.4}$$

$$V_{GT} := \sum_{i=1}^{n} \frac{1}{x'_{d_i}}\left[ \frac{V_i^2}{2} - E_i V_i \cos(\delta_i - \vartheta_i) \right] \tag{4.5}$$

$$V_{TT} := \sum_{i<j}^{n} B_{ij}\left[ \frac{V_i^2 + V_j^2}{2} - V_i V_j \cos(\vartheta_i - \vartheta_j) \right] + \sum_{i=1}^{n} B_{i,n+1}\left[ \frac{V_i^2}{2} - V_i \cos(\vartheta_i) \right] \tag{4.6}$$

$$V_{TL} := \sum_{i=1}^{n} \sum_{k=n+2}^{n+m+1} B_{ik}\left[ \frac{V_i^2 + V_k^2}{2} - V_i V_k \cos(\vartheta_i - \varphi_k) \right] +$$

$$\sum_{k=n+2}^{n+m+1} B_{k,n+1}\left[\frac{V_k^2}{2} - V_k \cos(\varphi_k)\right] \tag{4.7}$$

$$V_{LL} := \sum_{k<l}^{n+m+1} B_{kl}\left[\frac{V_k^2 + V_l^2}{2} - V_k V_l \cos(\varphi_k - \varphi_l)\right] \tag{4.8}$$

Here G stands for the internal and T for the terminal generator buses, and L for the load buses. Similar re-grouping can be carried out for the energy function of the one-axis model.

During a fault large amounts of energy are transferred from one system component (generator, line, load) to another. We give an example that shows this transfer of energy, during and after a fault, for the stable and unstable case. The network is shown in Figure 2 and its data are given in Section 6 (Table 1, 2 and 3). Buses 8,9 and 10 are the internal and 4,5 and 6 the terminal generator buses. The fault occurs, at 0.04 sec, on the line connecting buses 3 and 5 at a distance of 25% (of the line) from bus 3. If the line recloses at 0.34 sec the system is stable, Figure 9, whereas at 0.36 sec generator 8 separates from the others as shown in Figure 10, and the system becomes unstable. The terms of the energy function are evaluated along the fault-on trajectory for both cases shifted by a constant so that their value at the stable equilibrium point is zero. The terms $V_{P_l}$, $V_{Q_l}$, $V_{TT}$, $V_{LL}$ are negligible in relation to $V_{kin}$, $V_{P_m}$, $V_{GT}$ and $V_{TL}$. The latter are shown in Figures 5 and 6 for the stable and unstable case respectively. Examining in detail both cases we found that, soon after the fault, the terminal voltage $V_4$ of generator 8 drops and the angle difference $\delta_8 - \vartheta_4$ increases. The dominant factor though is $\delta_8 - \vartheta_4$ which increases up to 80° making the $\cos(\delta_8 - \vartheta_4)$ term in $V_{GT}$ almost equal to zero. This is shown in Figure 3. The shape of the $V_{GT}$ curve is determined by this factor. Similarly the dominant factor in the term $V_{TL}$ is $\vartheta_5 - \varphi_3$ which is shown in Figure 4. Around 0.5 sec these angle differences are maximum. In the interval 0.8 - 1.2 sec the terminal

voltage as well as the differences $\delta_8 - \vartheta_4$ and $\vartheta_5 - \varphi_3$ are very close to their equilibrium value. As a result the energy function terms involving these variables are also close to zero. On the other hand $\delta_8$ is at its minimum causing the $V_{P_m}$ term to become maximum. By the time this maximum is reached all the kinetic energy has been transformed to potential energy. This is not true in the unstable case (Figure 6) where at no time does all the kinetic energy get transformed to potential energy. In almost all the faults that were simulated a similar pattern was observed. There is little energy transfer between the load buses ( $V_{LL}$ is very small ) and between the terminal generator buses ( $V_{TT}$ is also small ).

### 4.2. A Reformulation

We present a reformulation of the energy function that greatly simplifies its computation.

Consider the one-axis model and its energy function $W_1$ as given by (3.15). In practice it is also customary to have $W_1 = 0$ at the stable equilibrium by subtracting from $W_1$ its value at the equilibrium. Let $(\delta^s, E'^s_q, \vartheta^s, V^s, \varphi^s)$ denote the stable equilibrium. Using (3.7) and (3.9) we can rewrite $W_1$ as follows

$$W_1(\omega, \delta, E'_q, \vartheta, V, \varphi) = \frac{1}{2}(2\pi f)<(\omega-1), M(\omega-1)> - <P^m, \delta-\delta^s> +$$

$$\frac{1}{2}\sum_{i=1}^{n}\left[\frac{x_{d_i}}{x'_{d_i}(x_{d_i}-x'_{d_i})}E'^2_{q_i} - \frac{1}{x'_{d_i}}\left[E'_{q_i}V_i\cos(\delta_i-\vartheta_i)\right]\right] -$$

$$\frac{1}{2}\sum_{i=1}^{n}\left[\frac{x_{d_i}}{x'_{d_i}(x_{d_i}-x'_{d_i})}E'^{s2}_{q_i} - \frac{1}{x'_{d_i}}\left[E'^s_{q_i}V^s_i\cos(\delta^s_i-\vartheta^s_i)\right]\right] -$$

$$<\frac{1}{x_d-x'_d}E_F, E'_q-E'^s_q> + \frac{1}{2}(Q_{n+1}-Q^s_{n+1}) -$$

$$<P^d,\varphi-\varphi^s> - <Q^d,\log\frac{V}{V^s}> \qquad (4.9)$$

Similarly, for the classical model,

$$W_2(\omega,\delta,\vartheta,V,\varphi) = \frac{1}{2}(2\pi f)<(\omega-1),M(\omega-1)> - <P^m,\delta-\delta^s> -$$

$$\frac{1}{2}\sum_{i=1}^{n}\frac{E_i}{x'_{d_i}}\left[V_i\cos(\delta_i-\vartheta_i) - V_i^s\cos(\delta_i^s-\vartheta_i^s)\right] +$$

$$\frac{1}{2}(Q_{n+1}-Q_{n+1}^s) - <P^d,\varphi-\varphi^s> - <Q^d,\log\frac{V}{V^s}> \qquad (4.10)$$

where $Q_{n+1}$ is the reactive power injection at the infinite bus which is not constant. If, instead of the $(n+1)^{st}$ terminal generator bus we take as infinite bus its internal generator bus, then

$$Q_{n+1}-Q_{n+1}^s = -\frac{1}{x'_{n+1}}[V_{n+1}\cos(\vartheta_{n+1}) - V_{n+1}^s\cos(\vartheta_{n+1}^s)],$$

otherwise we have to sum the reactive power flow from bus n+1 to all the buses that are connected to it.

The sum in (4.10) can also be written as

$$-\frac{1}{2}\sum_{i=1}^{n}\frac{E_i}{x'_{d_i}}\left[V_i\cos(\delta_i-\vartheta_i) - V_i^s\cos(\delta_i^s-\vartheta_i^s)\right] = \frac{1}{2}\sum_{i=1}^{n}(Q_i-Q_i^s)$$

where $Q_i$ is the reactive power injection at the $i^{th}$ generator internal bus. The same form is not possible for the corresponding sum in (4.9), but both functions (4.9) and (4.10) can take a simpler form.

The voltage behind synchronous reactance, $E_{F_i}$, is given by[5]

$$E_{F_i} = \frac{L_{AD_i} V_{F_i}}{r_{F_i}} \tag{4.11}$$

Using (2.7), (2.9), (3.19) and (4.11) we have

$$W_\alpha = \frac{1}{2}(2\pi f)<(\omega-1), M(\omega-1)> - <P^m, \delta-\delta^s> -$$

$$<\frac{1}{r_f} V_F, \Phi_F - \Phi_F^s> + \frac{1}{2}\sum_{i=1}^{n}[\Phi_{F_i} I_{F_i} - \Phi_{F_i}^s I_{F_i}^s] +$$

$$\frac{1}{2}(Q_{n+1} - Q_{n+1}^s) - <P^d, \varphi - \varphi^s> - <Q^d, \log \frac{V}{V^s}> \tag{4.12}$$

where $\alpha = 1$ or 2.

The time needed to compute $W_\alpha$ has been reduced substantially using (4.12) since the number of operations needed is proportional to the number of buses and is independent of how these buses are connected. Equation (4.12) is valid even if some or all of the terminal generator buses have local loads i.e. $P_i \neq 0$ and/or $Q_i \neq 0$.

Finally, the energy function (4.12) is a valid Lyapunov function for a power system where some of the generators, say those close to the fault location, are modeled with the one-axis model and the rest with the classical model.

[5] Depending on the choice of per unit base quantities a factor of $\sqrt{3}$ might be needed i.e. $\sqrt{3}E_{F_i} = \cdots$

## 5. Asymptotic Stability

Consider a power system where the generators are modeled with the classical model. The distinction between internal and terminal generator buses, although helpful in calculating the total energy function, is not needed for analysis. Therefore, we incorporate the terminal buses and the transient reactances into the bus admittance matrix. The resulting network is still lossless. The system model is then given by (cf. (3.21) - 3.33))

$$M\ddot{\delta} + D\dot{\delta} = P^m - f(\delta, \varphi, V) \tag{5.1}$$

$$0 = P^d - g(\delta, \varphi, V)) \tag{5.2a}$$

$$0 = Q^d - h(\delta, \varphi, V) \tag{5.2b}$$

where M and D have been normalized by $2\pi f$,

$$f_i(\delta, \varphi, V) = \sum_{j=1, j\neq i}^{n+1} E_i E_j B_{ij} \sin(\delta_i - \delta_j) + \sum_{k=n+2}^{n+m+1} E_i V_k B_{ik} \sin(\delta_i - \varphi_k)$$

and

$$P_k^d = g_k(\delta, \varphi, V) := \sum_{i=1}^{n+1} V_k E_i B_{ki} \sin(\varphi_k - \delta_i) + \sum_{l\neq k}^{n+m+1} V_k V_l B_{kl} \sin(\varphi_k - \varphi_l)$$

$$Q_k^d = h_k(\delta, \varphi, V) := -B_{kk} V_k^2 - \sum_{i=1}^{n+1} V_k E_i B_{ki} \cos(\varphi_k - \delta_i) - \sum_{l\neq k}^{n+m+1} V_k V_l B_{kl} \cos(\varphi_k - \varphi_l)$$

The energy function is given by

$$W_2(\dot{\delta}, \delta, \varphi, \nu) = \frac{1}{2}\dot{\delta}^T M \dot{\delta} + V_2(\delta, \varphi, \nu) \tag{5.3}$$

where $\nu_k = \log V_k$, $k = n+2,\ldots,n+m+1$, and

$$V_2(\delta,\varphi,\nu) = -\langle P^m,\delta\rangle - \langle P^d,\varphi\rangle - \langle Q^d,\nu\rangle - \sum_{i<j}^{n+1} B_{ij}E_iE_j\cos(\delta_i-\delta_j) - \sum_{i=1}^{n+1}\sum_{k=n+2}^{n+m+1} B_{ik}E_i e^{\nu_k}\cos(\delta_i-\varphi_k) - \sum_{k<l}^{n+m+1} B_{kl}e^{\nu_k+\nu_l}\cos(\varphi_k-\varphi_l) - \sum_{k=n+2}^{n+m+1} B_{kk}\frac{e^{2\nu_k}}{2} \qquad (5.4)$$

and

$$\frac{d}{dt}W_2(\dot\delta,\delta,\varphi,\nu) = -\dot\delta^T D\dot\delta \le 0 \qquad (5.5)$$

Recall that an equilibrium is (asymptotically) stable if trajectories starting at initial states sufficiently close to the equilibrium converge to it. Since (5.3) is decreasing along (continuous) trajectories, we have

**Lemma 5.1**

An equilibrium $(\delta^0,\varphi^0,V^0)$ is stable iff it is a local minimum of the potential $V_2$ (restricted to the surface $\Sigma_3$ defined by (5.2)) i.e. iff $P^TF_2P$, evaluated at $(\delta^0,\varphi^0,V^0)$ is positive definite, where P is the projection of $(\delta,\varphi,V)$ on $\Sigma_3$ and $F_2$ is the Hessian of $V_2$.

There is a very simple sufficient condition for stability if there are no load-to-load connections i.e. if power transfer through lines connecting loads can be neglected.

**Lemma 5.2**

Consider a power system modeled with the classical model (5.1) - (5.2). Assume that there are no load-to-load connections i.e. $B_{kl} = 0$ and let $(\delta^0,\varphi^0,V^0)$ be an equilibrium. If

1) $|\delta_i^0 - \delta_j^0| < \frac{\pi}{2}$, whenever $B_{ij} > 0$, $i,j = 1,\ldots,n$

2) $\cos(\delta_i^0 - \varphi_k^0) \geq \frac{E_i}{2V_k^0}$, whenever $B_{ik} > 0$, $i = 1,\ldots,n$, $k = n+2,\ldots,n+m+1$

Then $(\delta^0, \varphi^0, V^0)$ is asymptotically stable.

**Proof** see Appendix

Condition (2) of Lemma 5.2 has appeared in the literature, see [36], as an assumption in the form $2V_k > E_i$. As far as we know this is the first time that some physical interpretation is given to it.

We emphasize that these conditions are only sufficient. In Section 7 we give an example with two stable equilibrium points and in one of them these conditions are violated.

We give now some theoretical results concerning the region of attraction of a stable equilibrium point. In the interest of brevity let x denote the state of the system (x is $(\dot{\delta}, \delta)$ for the classical model and $(\dot{\delta}, \delta, E'_q)$ for the one-axis model). The algebraic equations have been solved for the non-state variables in terms of x. The model then can be expressed as

$$\dot{x} = F(x)$$

Consider the classical model. Notice that the sets $\{V_2 < c\}$ and $\{W_2 < c\}$ are not bounded so the next result is surprising.

**Lemma 5.3**

Let A be any (positively) invariant set of the state space and $c_1 < c_2$ be such that $c_1 \leq W_1(\dot{\delta}, \delta) \leq c_2$ for $(\dot{\delta}, \delta)$ in A. Then A is bounded. (Invariant means that a trajectory starting in A cannot leave A.)

**Proof** see Appendix

The analogous result holds for the one-axis model. Since (3.3) is linear in $E'_q$ and has a bounded input it follows that $E'_q$ is bounded as well. The rest of the argument is identical to the proof for the classical model.

We are concerned with the region of attraction of a stable equilibrium point, say $x^0$. Let $\Phi(t, x)$ denote the state at time t starting in state x at time 0. Then

$$A := \{x \mid \Phi(t, x) \to x^0 \text{ as } t \to \infty\}$$

is the **attractor** (or region of attraction) of $x^0$. Our aim is to characterize A by describing its boundary.

Assume that the equilibrium points are hyperbolic i.e. the Jacobian of F(x) at these points has no imaginary eigenvalues.

Let

$\partial A$ , $\bar{A}$ = the boundary and closure of A respectively,

ind(x) = the index of a hyperbolic fixed point x, i.e.
the number of eigenvalues with positive real part,

$M^s(x)$ = the stable manifold of $x = \{y \mid \Phi(t,y) \to x \text{ as } t \to \infty\}$,

$M^u(x)$ = the unstable manifold of $x = \{y \mid \Phi(t,y) \to x \text{ as } t \to -\infty\}$.

Note that ind(x) is equal to the dimension of $M^u(x)$. The following result is well known.

**Lemma 5.4**

The boundary of A, $\partial A$, is invariant.

Let W (equal $W_1$ or $W_2$ ) denote the appropriate energy function. Let $x \in \partial A$. Then $W(x) > W(x^0)$. Since W decreases along trajectories, $W(\Phi(x,t)) < W(x)$. By Lemma 5.3 the trajectory $\Phi(x,t)$ is bounded, hence it must converge to some equilibrium $x_i \in \partial A$. Hence

$$\partial A \subset \bigcup_i M^s(x_i) \tag{5.6}$$

where i ranges over all equilibrium points $x_i \in \partial A$. These equilibria must be unstable i.e. $\text{ind}(x_i) \geq 1$. Since the stable manifold of any $x_i$ with $\text{ind}(x_i) > 1$ is of lower dimension (hence nowhere dense), by use of the Baire category theorem, (5.6) implies

$$\partial A \subset \bigcup_i \overline{M^s(x_i)} \tag{5.7}$$

where i ranges over the $x_i$ with $\text{ind}(x_i) = 1$.

To investigate whether equality hold in (5.6) or (5.7) we need the following Lemma.

**Lemma 5.5**

Let $x_i \in \partial A$ be a hyperbolic equilibrium point. If $M^u(x_i) \cap A \neq \phi$ then $M^s(x_i) \subset \partial A$.

**Proof** see Appendix

If $x_i \in \partial A$, it can be shown that $M^u(x_i)$ contains points $z \in \bar{A}$, $z \neq x_i$. Suppose that $z \in \partial A$. Because of (5.6) z must be on the stable manifold of some $x_j \in \partial A$, $x_j \neq x_i$, which implies the next result.

**Theorem 5.1**

If

$$\left\{ M^u(x_i) \cap M^s(x_j) \right\} \cap \partial A = \phi \tag{5.8}$$

for $x_i$, $x_j$ on $\partial A$, $x_i \neq x_j$, $\text{ind}(x_i) = 1$, then

$$\partial A = \bigcup_i \overline{M^s(x_i)},$$

where i ranges over the $x_i \in \partial A$, with $\text{ind}(x_i) = 1$.

This result is the basis for our proposal to evaluate the critical clearing time presented in the next section.

One case where condition (5.8) fails is when a trajectory connects two saddle points as in Figure 7.

For each $c > 0$ let $A_c$ denote the component of the set $\{ x \mid W(x) < W(x^0) + c \}$ which contains $x^0$. Let $\bar{c}$ be the smallest value of c such that $A_c$ contains another equilibrium point $x^u$ on its boundary.

**Theorem 5.2**

$A_{\bar{c}} \subset A$. Moreover $x^u$ is an unstable equilibrium on the boundary of A.

**Proof** see Appendix

**Corollary 5.1**

$A_{\bar{c}}$ is the only bounded component of the set $\{ W(x) < W(x^0) + \bar{c} \}$.

These two results together give the behavior suggested by Figure 8.

## 6. Critical Clearing Time Evaluation

Lyapunov's direct method can be used effectively in power systems for on-line stability analysis. Although its use has been limited to small systems and the reported results are considered conservative, we believe that the energy functions defined above, especially in their simplified form, are suitable for large systems since they require very little computation time.

The situation to be studied here can be described briefly as follows. Initially the system is operating at a stable equilibrium $x^0$. At time $t_0$ a fault occurs and the system moves away from $x^0$ governed by the dynamics of the faulted system. At some time later $t_1$ the fault is cleared. Let $x^1$ be the state at $t_1$ and $x^{00}$ a stable equilibrium of the post-fault system. The question of interest is to determine whether or not the trajectory of the post-fault system starting at $x^1$ converges to $x^{00}$.

**Remark 6.1**

In practice $x^1$ is not known since monitoring of the state is impractical. Hence it must be estimated from the pre-fault equilibrium state $x^0$ and the dynamics of the faulted system. In principle $x^1$ can be calculated by integrating the equations of the latter, over the fault-on period, starting from $x^0$. The system is too large and the available time too short for this to be practical and some approximations must be made [16].

The time period $t_1 - t_0$ is the fault clearing time, $t_{cl}$. The maximum $t_{cl}$ such that the post-fault trajectory converges to $x^{00}$ is defined as the **critical clearing time**, $t_{cr}$. The value of the energy function at $t = t_{cr}$ is denoted by $W_{cr}$.

Many techniques have been developed for the evaluation of $t_{cr}$ based on $W_{cr}$. The motivation for most of them comes from the "equal area criterion" for the

case of one machine connected to an infinite bus, see [7,16]. All of them assume knowledge of the post-fault network.

One method for evaluating $t_{cr}$ for multimachine systems, based on the "equal area criterion", can be described as follows. A sustained fault is simulated and the post-fault potential energy function V is evaluated along the trajectory of the faulted system. Its maximum value, $V_{max}$, is noted and saved. When a fault occurs the post-fault total energy function W is evaluated along the trajectory of the faulted system. The critical clearing time is estimated to be the time when $W(x(t_{cr})) = V_{max}$. We will refer to this method as the total energy method.

The technique proposed in [29] is identical to the previous method except that, instead of the energy function of the whole system, the so-called "individual energy function" of a critical machine is used. A critical machine (or critical group of machines) is defined as the generator which tends to separate from the rest of the generators soon after the fault. Although such individual energy functions are not Lyapunov functions the idea seems interesting. Motivated by it we define the individual potential and total energy function of the $i^{th}$ generator as

$$W_i = \frac{1}{2}(2\pi f)M_i(\omega_i-1)^2 + V_i \tag{6.1}$$

where, for the one-axis model,

$$V_i = -P_i^m\delta_i - \frac{E_{F_i}}{x_{d_i}-x'_{d_i}}E'_{q_i} - \frac{E'_{q_i}V_i\cos(\delta_i-\vartheta_i)}{x'_{d_i}} -$$

$$\left[B_{ii} + \frac{(x'_{d_i}-x_{q_i})\cos[2(\delta_i-\vartheta_i)] - (x'_{d_i}-x_{q_i})}{2x_{q_i}x'_{d_i}}\right]\frac{V_i^2}{2} +$$

$$\frac{x_{d_i}}{x'_{d_i}(x_{d_i}-x'_{d_i})}\frac{E'^2_{q_i}}{2} - \sum_{j\neq i}^{n+1}B_{ij}V_iV_j\cos(\vartheta_i-\vartheta_j) -$$

$$\sum_{k=n+2}^{n+m+1} B_{ik} V_i V_k \cos(\vartheta_i - \varphi_k) \tag{6.2}$$

and, for the classical model,

$$V_i = -P_i^m \delta_i - \frac{E'_{q_i} V_i \cos(\delta_i - \vartheta_i)}{x'_{d_i}} - (B_{ii} - \frac{1}{x'_{d_i}}) \frac{V_i^2}{2} -$$

$$\sum_{j \neq i}^{n+1} B_{ij} V_i V_j \cos(\vartheta_i - \vartheta_j) - \sum_{k=n+2}^{n+m+1} B_{ik} V_i V_k \cos(\vartheta_i - \varphi_k) \tag{6.3}$$

Note that the sum of the individual energy functions is *not equal* to the whole system energy function. As in the total energy function, (6.2) and (6.3) can also take a simplified form, namely

$$V_i = -P_i^m \delta_i - \frac{E_{F_i}}{x_{d_i} - x'_{d_i}} E'_{q_i} + \frac{x_{d_i}}{x'_{d_i}(x_{d_i} - x'_{d_i})} \frac{E'^2_{q_i}}{2} +$$

$$\left[ B_{ii} + \frac{(x'_{d_i} - x_{q_i}) \cos[2(\delta_i - \vartheta_i)] - (x'_{d_i} - x_{q_i})}{2 x_{q_i} x'_{d_i}} \right] \frac{V_i^2}{2} \tag{6.6}$$

for the one-axis model, and

$$V_i = -P_i^m \delta_i + (B_{ii} - \frac{1}{x'_{d_i}}) \frac{V_i^2}{2} \tag{6.7}$$

for the classical model.

We will refer to this approach as the **individual energy** method.

One drawback of these methods is that they are fault-dependant since $V_{max}$ differs from fault to fault so that a separate simulation has to be carried out for

each fault. Moreover the potential function (individual or total) may not have a maximum value. In the next section we give such an example.

The method we propose here differs from the two previous methods. We assume that a load flow study has been performed to determine the unstable equilibrium points of the post-fault system and the value of the total (potential) energy function at each of these points (in the case when the post-fault and pre-fault network are the same no extra computation effort is needed, during the fault-on period, to obtain these values). The total energy function of the post-fault system is then evaluated along the trajectory of the fault-on system together with the distance of the state from each of the unstable equilibrium points (u.e.p.'s). By distance we mean the Euclidean distance in S' (or S) i.e.

$$\left[\sum_{i=1}^{n} |\delta_i(t) - \delta_i^u|^2\right]^{1/2} \quad \text{for the classical model,}$$

and

$$\left[\sum_{i=1}^{n} (|\delta_i(t) - \delta_i^u|^2 + |E'_{q_i}(t) - E'^u_{q_i}|^2\right]^{1/2} \quad \text{for the one-axis model,}$$

where $\delta^u$ (or $(\delta^u, E'^u_q)$) denotes the unstable equilibrium. The equilibrium point with the minimum distance is called the closest u.e.p.. The critical clearing time is defined as the time when the value of the total energy function is equal to its value at the closest u.e.p..

The intuition behind this method comes from the theoretical results in Section 5. From Theorem 5.1 we see that if the faulted trajectory leaves the attractor A of $x^{00}$, then it must "pierce" the boundary $\partial A$ at some point, say x. Moreover x must belong to the stable manifold of an unstable equilibrium, say $x^u$.

Then $W(x) \geq W(x^u)$ and $x^u$ is likely to be the closest u.e.p.. The critical clearing time estimated by $W(x^u)$ will then be smaller than the true critical clearing time, and the approximation will be better the closer is x to $x^u$.

We will refer to this method as the closest u.e.p. method.

**Remark 6.2**

As was mentioned in the beginning of this Section, for on-line analysis, the available time is too short to calculate all the u.e.p.'s, especially for large systems. There are methods which try to determine the closest u.e.p., and hence $V_{cr}$, by merely observing the generator (or group of generators) that accelerates after the fault, see [16,22]. But there can be many such equilibria and it is not clear which one of them should be chosen. We believe that a combination of these approximate methods and the closest u.e.p. method will result in a more feasible method for on-line transient stability analysis.

## 7. Examples

The 10-bus, 4-machine system of Figure 2 is taken from Pai [16] with some modifications. Tables 1 and 2 give the line and model data, respectively. Only the classical model is considered. Buses 8,9 and 10 are the internal buses and 4,5,6 are the corresponding terminal generator buses. They are connected through the transient reactance $x'_d$. Bus 7 is the infinite bus i.e. $V_7 = 1.0$ and $\vartheta_7 = 0.0$. Table 3 gives the specified initial data.

Using the simulation program described in [27], we find eight equilibrium points of which **two (!)** are stable and six are unstable. They can be separated in two classes, each containing one stable and three unstable ones. In the first class $V_1$ is close to 1.0 p.u. In the second class $V_1$ is very low. The equilibria are shown in Tables 4 and 5 along with the value of the Lyapunov (Energy) function.

| LINE DATA | | |
|---|---|---|
| From bus | To bus | Susceptance (p.u) |
| 1 | 2 | −2.500 |
| 1 | 3 | −2.000 |
| 1 | 6 | −3.333 |
| 2 | 7 | −6.666 |
| 3 | 4 | −3.000 |
| 3 | 5 | −2.000 |
| 3 | 7 | −5.000 |
| 4 | 8 | −1.000 |
| 5 | 6 | −1.250 |
| 5 | 9 | −2.000 |
| 6 | 10 | −2.500 |

**Table 1.**

| GENERATOR MODEL DATA | | | |
|---|---|---|---|
| Number | $x'_d$ (p.u) | M (p.u) | D (p.u) |
| 8 | 1.0 | 1,130.0 | 1.130 |
| 9 | 0.5 | 2,260.0 | 2.260 |
| 10 | 0.4 | 1,508.0 | 1.508 |

**Table 2.**

| SPECIFIED INITIAL DATA ( p.u. ) | | | | | |
|---|---|---|---|---|---|
| Generators | | | Loads | | |
| Bus | $P_m$ | $E'_q$ | Bus | P | Q |
| 8 | 0.4 | 1.057 | 1 | −0.5 | −0.15 |
| 9 | 0.5 | 1.155 | 2 | −0.3 | −0.10 |
| 10 | 0.3 | 1.095 | 3 | −0.2 | −0.10 |

**Table 3.**

| EQUILIBRIUM POINTS ( CLASS I ) | | | | |
|---|---|---|---|---|
| Bus | s.e.p. | | u.e.p. | |
| | Voltage | Angle | Voltage | Angle |
| 1 | 0.9722 | 0.4267 | 0.8969 | 0.6773 |
| 2 | 0.9807 | −1.8130 | 0.9599 | −1.8399 |
| 3 | 0.9790 | 4.7676 | 0.8091 | 5.7522 |
| 4 | 0.9703 | 12.8361 | 0.4328 | 28.1304 |
| 5 | 1.0389 | 14.7012 | 0.9577 | 18.1934 |
| 6 | 1.0197 | 8.2376 | 0.9678 | 9.9481 |
| 8 | 1.0570 | 35.7908 | 1.0570 | 147.1708 |
| 9 | 1.1550 | 26.7261 | 1.1550 | 31.2564 |
| 10 | 1.0950 | 14.4074 | 1.0950 | 16.4499 |
| V | 0.000000 | | 0.391133 | |
| Bus | u.e.p. | | u.e.p. | |
| | Voltage | Angle | Voltage | Angle |
| 1 | 0.7532 | 1.0982 | 0.6928 | 1.6640 |
| 2 | 0.9201 | −1.9436 | 0.9034 | −1.9232 |
| 3 | 0.7165 | 6.5401 | 0.5901 | 7.8335 |
| 4 | 0.7485 | 20.9355 | 0.3800 | 44.3175 |
| 5 | 0.2218 | 84.1014 | 0.2457 | 97.5104 |
| 6 | 0.7390 | 16.3981 | 0.7005 | 20.0431 |
| 8 | 1.0570 | 51.3055 | 1.0570 | 129.0612 |
| 9 | 1.1550 | 161.4618 | 1.1550 | 159.2609 |
| 10 | 1.0950 | 24.9266 | 1.0950 | 29.0437 |
| V | 1.093655 | | 1.196225 | |

**Table 4.**

| EQUILIBRIUM POINTS ( CLASS II ) | | | | |
|---|---|---|---|---|
| Bus | s.e.p. | | u.e.p. | |
| | Voltage | Angle | Voltage | Angle |
| 1 | 0.1302 | −41.2120 | 0.1542 | −32.2850 |
| 2 | 0.7383 | −5.1465 | 0.7473 | −4.9764 |
| 3 | 0.6900 | 10.7167 | 0.5631 | 12.9751 |
| 4 | 0.7240 | 26.1983 | 0.3861 | 50.7972 |
| 5 | 0.7577 | 44.6052 | 0.6780 | 59.6531 |
| 6 | 0.5026 | 54.6438 | 0.4826 | 67.4522 |
| 8 | 1.0570 | 57.7129 | 1.0570 | 129.3304 |
| 9 | 1.1550 | 61.2043 | 1.1550 | 78.2704 |
| 10 | 1.0950 | 67.2385 | 1.0950 | 80.5762 |
| V | 1.302421 | | 1.379109 | |
| Bus | u.e.p. | | u.e.p. | |
| | Voltage | Angle | Voltage | Angle |
| 1 | 0.2825 | −6.3762 | 0.2815 | −5.7765 |
| 2 | 0.7890 | −3.5676 | 0.7888 | −3.5101 |
| 3 | 0.5478 | 11.0993 | 0.5068 | 11.8871 |
| 4 | 0.5685 | 36.4473 | 0.4422 | 48.3988 |
| 5 | 0.4005 | 117.8124 | 0.4173 | 116.9271 |
| 6 | 0.4114 | 95.0313 | 0.4214 | 92.3404 |
| 8 | 1.0570 | 78.1796 | 1.0570 | 107.2494 |
| 9 | 1.1550 | 150.5276 | 1.1550 | 148.1679 |
| 10 | 1.0950 | 110.4815 | 1.0950 | 107.4123 |
| V | 1.424024 | | 1.428421 | |

**Table 5.**

Only line faults are simulated. If the line connecting buses i and j trips then the faulted network has that line removed and a shunt inductance is inserted at each of the buses i, j the value of which depends on the location of the fault. Clearing the fault means that the buses are re-connected and the shunts removed, so the pre-fault and the post-fault networks are the same. In all the cases the fault occurs at 0.04 sec so the pre-fault values of the variables are also shown. The location of the fault is given as a percentage of the distance (as measured from the first bus) between the two buses that specify the line. Table 6 shows the critical clearing time for different faults obtained with the three methods. The integration step in the simulation program is 0.02 sec.

Two cases are analyzed explicitly.

**Example 7.1** : Line 3 - 5. Fault location 25% from bus 3.

The actual critical clearing time for this fault, obtained from simulations, is equal to **0.30 sec** as shown in Figure 9. If the fault clears after 0.32 sec the system becomes unstable *after* it survives the first swing (Figure 10), while after 0.34 sec generator 8 separates from the others in the first swing (Figure 11).

Figure 12 shows the generator angles when a sustained fault is simulated. The critical generators are 8 and 9. Their individual total and potential energy is shown in Figure 13 along with the total and potential energy of the whole system.

Using the individual energy method the estimated critical clearing time is equal to **0.40 sec** while the total energy method gives an estimate of **0.36 sec.**

Using the closest u.e.p. method the estimated critical clearing time is equal to **0.22 sec.**

We see that in this case the only reliable method is the closest u.e.p. method, although a little conservative. The other methods give wrong results.

| Fault | | Critical Clearing Time (sec) | | | |
|---|---|---|---|---|---|
| Line | Loc. | Individual Ener. Meth. | Total Ener. Meth. | Closest u.e.p. Meth. | Actual |
| 1 – 3 | 50% | NA | NA | 0.38 | 0.44 |
| 1 – 3 | 75% | 0.38 | 0.36 | 0.26 | 0.32 |
| 3 – 5 | 25% | 0.40 | 0.38 | 0.22 | 0.30 |
| 3 – 5 | 50% | 0.40 | 0.38 | 0.22 | 0.38 |
| 3 – 5 | 75% | 0.34 | 0.32 | 0.20 | 0.34 |
| 5 – 6 | 25% | 0.48 | 0.46 | 0.46 | 0.46 |
| 5 – 6 | 50% | 0.80 | 0.78 | 0.78 | 0.78 |
| 5 – 6 | 95% | NA | NA | 0.24 | 0.42 |
| 1 – 6 | 95% | NA | NA | 0.20 | 0.34 |

**Table 6.**

**Example 7.2** : Line 1 - 6. Fault location 95% from bus 1.

The actual critical clearing time for this fault, obtained from simulations, is equal to **0.34 sec** as shown in Figure 14.

A sustained fault is simulated. Figure 15 shows the generator angles. But neither the individual potential energy of the critical generator 10 nor the individual energy of any other generator reaches a maximum. The same is true for the potential energy of the whole system as it is shown in Figure 16. Therefore, the previously mentioned methods are not applicable (NA) to estimate the critical clearing time.

Using the closest u.e.p. method the estimated critical clearing time is equal to **0.20 sec.**

The rest of the fault cases are shown in Table 6.

**Remark 7.1**

The results in this Section indicate that methods using $V_{max}$ as the critical energy can give critical clearing time larger than the actual one. The closest u.e.p. method is more reliable although in some cases the estimated critical clearing time is conservative. Closer examination reveals that in all of these cases for some time after the fault the closest u.e.p. is also the u.e.p. with the smallest energy. It is this u.e.p. that determines the critical clearing time. At some time later the closest u.e.p. changes and the value of the energy function is smaller than its value at the new u.e.p.. Applying the method again the estimated critical clearing time is very close (sometimes equal) to the actual clearing time.

**Remark 7.2**

Instability can occur even if the system survives the first swing. Example 7.1 contradicts an implicit assumption made in previous stability analyses that are based on the intuition gained from the equal area criterion.

## APPENDIX

**Proof of Lemma 5.2**

Let $x \in R^n$ and $y, z \in R^m$ be any vectors and consider the product $(x, y, z)^T F_2 (x, y, z)$. After collecting terms and forming the squares we have

$$(x, y, z)^T F_2 (x, y, z) = S_{gg} + S_{gl}$$

where, after replacing $e^{\nu_k}$ with $V_k$,

$$S_{gg} = \sum_{i=1}^{n} \sum_{j=i+1}^{n+1} E_i E_j B_{ij} \cos(\delta_i - \delta_j) (x_i - x_j)^2$$

$$S_{gl} = \sum_{i=1}^{n+1} \sum_{k=n+2}^{n+m+1} B_{ik} V_k \left\{ E_i \cos(\delta_i - \varphi_k) (x_i - y_k)^2 + \left[ 2V_k - E_i \cos(\delta_i - \varphi_k) \right] z_k^2 \right.$$

$$\left. + E_i \sin(\delta_i - \varphi_k) \left[ 2(x_i - y_k) z_k \right] \right\}$$

with $x_{n+1} \equiv 0$.

Hence, $F_2$ is positive definite if each of the two sums is nonnegative for all $(x, y, z) \in R^{n+2m+1}$ with at least one sum strictly positive.

A sufficient condition for $S_{gg} > 0$ is

$$|\delta_i - \delta_j| < \frac{\pi}{2} \qquad \text{whenever} \quad B_{ij} > 0.$$

Recall that a necessary and sufficient condition for $ax^2 + 2bxy + cy^2$ to be nonnegative is

1) $a > 0$

2) $ac \geq b^2$

Hence, each term in the sum of $S_{gl}$ is nonnegative iff

3) $\cos(\delta_i - \varphi_k) > 0$

4) $E_i \cos(\delta_i - \varphi_k) [\, 2V_k - E_i \cos(\delta_i - \varphi_k) \,] \geq E_i^2 \sin^2(\delta_i - \varphi_k)$

or, equivalently,

4') $\cos(\delta_i - \varphi_k) \geq \dfrac{E_i}{2V_k}$

Note that (4') implies (3). Therefore, a sufficient condition for $S_{gl} \geq 0$ for all $(x, y, z) \in R^{n+2m+1}$ is

$$\cos(\delta_i - \varphi_k) \geq \frac{E_i}{2V_k} \qquad \text{whenevr} \quad B_{ik} > 0.$$

**Proof of Lemma 5.3**

Limit attention to trajectories in A. Since $\frac{1}{2}\, \dot{\delta}^T M\, \dot{\delta} \leq W_1(\dot{\delta}, \delta) \leq c_2$ it follows that $\dot{\delta}(t)$ is uniformly bounded, and it only remains to show that $\delta(t)$ is uniformly bounded as well.

Differentiation of (5.1) reveals that $\dddot{\delta}(t)$ is uniformly bounded. For positive t, h Taylor's theorem applied to $\dot{\delta}$ implies

$$\dot{\delta}(t+h) - \dot{\delta}(t) - h\, \ddot{\delta}(t) = \tfrac{1}{2} h^2\, \xi$$

where $\xi_i := \delta_i(t+s_i)$ for some $0 \leq s_i \leq h$. Multiply both sides by M and use (5.1)

to get

$$M\,\dot{\delta}(t+h) - [\,M - h\,D\,]\,\dot{\delta}(t) = h\,[\,P^m - f(\delta(t))] + \tfrac{1}{2}\,h^2\,M\,\xi.$$

Hence there are positive constants $k_1$, $k_2$ such that for all small h

$$|\,\dot{\delta}(t+h)\,| + |\,\dot{\delta}(t)\,| \geq k_1\,h\,[\,|\,P^m - f(\delta(t))\,| - h\,k_2\,]. \tag{A.1}$$

(Here $|\ |$ denotes Euclidean norm.)

Let $E := \{\delta^0 \mid P^m - f(\delta^0) = 0\}$ be the set of equilibria. Let $B_\varepsilon(\delta^0)$ be the ball with radius $\varepsilon$ and center $\delta^0$. Choose $\varepsilon > 0$, $\eta > 0$ so that the distance between two different $B_\varepsilon(\delta^0)$ is at least $\varepsilon$ and $|\,P^m - f(\delta)\,| > \eta$ whenever $\delta \in \bigcup_E B_\varepsilon(\delta^0)$. For any trajectory let $T_\varepsilon := \{\, t \mid \delta(t) \in \bigcup_E B_\varepsilon(\delta^0)\,\}$ and let $L(T_\varepsilon)$ be its Lebesgue measure.

Suppose $\delta(t)$ is not uniformly bounded. Then $L(T_\varepsilon)$ cannot be bounded either.

By hypothesis A is invariant, and so, by (5.5),

$$\int_{T_\varepsilon} \dot{\delta}(t)^T\,D\,\dot{\delta}(t) \leq \int_0^\infty \dot{\delta}(t)^T\,D\,\dot{\delta}(t) \leq c_2 - c_1. \tag{A.2}$$

Let $d = \min D_i$ and take $h = \tfrac{1}{2}\,\eta\,k_2^{-1}$. Then, from (A.1) and (A.2)

$$2(c_2 - c_1) \geq 2\int_{T_\varepsilon} \dot{\delta}(t)^T\,D\,\dot{\delta}(t)\,dt \geq 2d\,[\,\tfrac{1}{4}\,k_1\,\eta^2\,k_2^{-1}\,]^2\,L(T_\varepsilon)$$

so that $L(T_\varepsilon)$ is uniformly bounded.

**Proof of Lemma 5.5**

Suppose $M^s(x_i) \not\subset \partial A$. Obviously $M^s(x_i) \cap A = \phi$. Hence there exist points $z \in M^s(x_i)$ such that $z \in (\bar{A})^c$ (compliment of $\bar{A}$). Take a small neighborhood V of z and consider $\bigcup_{t>0} \Phi(t,V)$, the orbit of V. Since $(\bar{A})^c$ is invariant, the orbit is an open subset of $(\bar{A})^c$. On the other hand, see [24], we have $\overline{\bigcup_{t>0} \Phi(t,V)} \supset M^u(x_i)$. Hence $M^u(x_i) \subset \overline{((\bar{A})^c)} = A^c$ which contradicts the hypothesis $M^u(x_i) \cap A \neq \phi$.

**Proof of Theorem 5.2**

It is not difficult to see using Lemma 5.1 that $W(x^0) \leq W(x)$ for x in $A_c$. Since W(x(t)) is decreasing, $A_c$ is invariant and then by Lemma 5.3 $A_c$ is bounded. Hence every trajectory in $A_c$ has at least one limit point, say $\bar{x}$. From (3.17) or (3.26) $\bar{x}$ must be an equilibrium and so, by construction, $\bar{x} = x^0$. So $A_c \subset A$. Finally, if $x^u$ were stable, then it would have an open attractor contradicting the fact that it is in $\partial A_c \subset \bar{A}$.

## REFERENCES

[1] Anderson, P. M. and A. A. Fouad, **Power System Control and Stability, Volume 1.** The Iowa State University Press, Ames, Iowa, 1977.

[2] Arapostathis, A., S. Sastry and P. Varaiya, "Analysis of the Power Flow Equations", *Electrical Energy and Power Systems*, vol. 3(3), pp. 115-126, 1981.

[3] Arapostathis, A., S. Sastry, P. Varaiya, "Global Analysis of Swing Dynamics", *IEEE Transactions on Circuits and Systems*, vol. CAS-29(10), Oct. 1982, pp. 673-679.

[4] Arapostathis, and P. Varaiya, "The Behavior of Three Node Power Networks", *Electrical Energy and Power Systems*, vol. 5(1), Jan. 1983, pp. 22-29.

[5] Athay, T., R. Podmore and S. Virmani, "A Practical Method for the Direct Analysis of Transient Stability", *IEEE Transactions on Power Apparatus and Systems*, vol. PAS-98, pp. 573-584, 1979.

[6] Athay, T. and D. I. Sun "An Improved Energy Function for Transient Stability Analysis", Proc. International Symposium on Circuits and Systems, April 27-29, 1981, Chicago.

[7] Aylett, P. D., "The Energy Integral Criterion of Transient Stability Limits of Power Systems", *Proceedings IEE (London)*, vol. 105(C),

pp. 527-536, 1958.

[8] Bergen, A. R. and D. J. Hill, "A Structure Preserving Model for Power System Stability Analysis", *IEEE Transactions on Power Apparatus and Systems*, vol. PAS-100 (1981), pp. 25-35.

[9] El-Abiad, A. H. and K. Nagappan, "Transient Stability Regions of Multimachine Power Systems", *IEEE Transactions on Power Apparatus and Systems*, vol. PAS-85 (1966), pp. 169-179.

[10] Fouad, A. A., "Stability Theory - Criteria for Transient Stability", in *Systems Engineering of Power: Status and Prospects* (ed. L. H. Fink and K. Carlson), U.S. ERDA and ERPI, 1975, pp. 421-450.

[11] Fouad, A. A. and S. E. Stanton, "Transient Stability of a Multimachine Power System, Part I: Investigation of System Trajectories; Part II: Critical Transient Energy", *IEEE Transactions on Power Apparatus and Systems*, vol. PAS-100 (1981), pp. 3408-3424.

[12] Gupta, C. L. and A. H. El-Abiad, "Determination of the Closest Unstable Equilibrium State for Lyapunov Methods in Transient Stability Studies", *IEEE Transactions on Power Apparatus and Systems*, vol. PAS-94 (1976), pp. 1699-1712.

[13] Hahn, W., **Theory and Applications of Lyapunov's Direct Method**. Prentice Hall, Englewood Cliffs, N.J., 1963.

[14] Hartman, P., **Ordinary Differential Equations.** New York: Wiley, 1964.

[15] Narasimhamurthi, N., "Application of Minimum Loss Property of Resistive Networks to Power Rescheduling" *IEEE Trans. on Circuits and Systems*, vol. CAS-29(11), Nov. 1981, pp. 775-777.

[16] Pai, M. A., **Power System Stability Analysis by the Direct Method of Lyapunov.** North Holland Systems and Control Series, Vol.3, 1981.

[17] Pai, M. A. and V. Rai, "Lyapunov-Popov Stability Analysis of Synchronous Machine with Flux Decay and Voltage Regulator", *International Journal of Control*, vol. 20(2), pp. 203-212, Aug. 1974.

[18] Padiyar, K. R. and P. Varaiya, "A Network Analogy for Power System Stability Analysis", *preprint*, Dec. 1983.

[19] Prabhakara, F. S. and A. H. El-Abiad, "A Simplified Determination of Transient Stability Regions for Lyapunov Methods", *IEEE Transactions on Power Apparatus and Systems*, vol. PAS-94 (1975), pp. 672-689.

[20] Ribbens-Pavella, M. "Critical Survey of Transient Stability Studies of Multimachine Power Systems by Lyapunov's Direct Method", *Proc. 9th Allerton Conf. on Circuit and System Theory*, October 6-8, 1971,pp.751-761.

[21] Ribbens-Pavella, M., Comments on J. L. Willems "Direct Methods for Transient Stability Studies in Power System Analysis", and Reply by Author, *IEEE Trans. Automatic Control*, vol. AC-17, pp. 415-417, June 1972.

[22] Ribbens-Pavella, M., A. Calvaer and J. Gheury, "Transient Stability Index for On-Line Evaluation", IEEE PES Winter Meeting, New York, NY, February 3-8, 1980.

[23] Sastry, S. and C. A. Desoer, "Jump Behavior of Circuits and Systems", *IEEE Trans. on Circuits and Systems*, vol. CAS-28(12), December 1981.

[24] Smale, S., "Differentiable Dynamical Systems", *Bull. Amer. Math. Soc.* 73, pp. 747-817, 1967.

[25] Tavora, C. J. and O. J. M. Smith, "Equilibrium Analysis of Power Systems", *IEEE Transactions on Power Apparatus and Systems*, vol. PAS-91 (1972), pp. 1131-1137.

[26] Tavora, C. J. and O. J. M. Smith, "Stability Analysis of Power Systems", *IEEE Transactions on Power Apparatus and Systems*, vol. PAS-91 (1972), pp. 1138-1144.

[27] Tsolas, N., "Stability and Computer Simulation of Power Systems", Ph.D. Dissertation, University of California, Berkeley, 1983.

[28] Vidyasagar, M., **Nonlinear Systems Analysis.** Prentice Hall, Englewood Cliffs, N.J., 1978.

[29] Vittal, V., "Power System Transient Stability Using Critical Energy of Individual Machines", Ph.D. Dissertation, Iowa State University, 1982.

[30] Willems, J. L., "The Computation of Finite Stability Regions by means of Open Lyapunov Surfaces", *Int. J. Control*, 1969, vol. 10, No. 5, pp. 537-544.

[31] Willems, J. L., "Optimum Lyapunov Functions and Stability Regions for Multimachine Power Systems", *Proceedings IEE*, Vol. 117, No. 3, March 1970, pp. 573-578.

[32] Willems, J. L. and J. C. Willems, "The Application of Lyapunov Methods to the Computation of Transient Stability Regions for Multimachine Power Systems", *IEEE Transactions on Power Apparatus and Systems*, vol. PAS-89, May/June 1970.

[33] Willems, J. L., "Direct Methods for Transient Stability Studies in Power System Analysis", *IEEE Trans. Automatic Control*, Vol. AC-16, No. 4, August 1971.

[34] Willems, J. L., "A Partial Stability Approach to the Problem of Transient Power System Stability", *Int. J. Control*, 1974, vol. 19, No. 1, pp. 1-14.

[35] Williams, H. F., S. A. Louie and G. W. Bills, "Feasibility of Lyapunov Functions for the Stability Analysis of Electric Power Systems having up to 60 Generators" *IEEE Transactions on Power Apparatus and Systems*, vol. PAS-91, May/June 1972, pp. 1145-1153.

[36] Wu, F. F. and S. Kumagai, "Steady-state Security Regions of Power Systems" *IEEE Transactions on Circuits and Systems*, vol. CAS-29, Nov. 1982, pp. 703-711.

[37] Wu, F., Lecture Notes for Course EECS 214, University of California, Berkeley, Spring 1981.

Figure Captions

1. Phasor diagram of stator for the one-axis model
2. Network for example
3. Significant phase angles in V
4. Significant phase angles in V
5. Components of energy for stable case
6. Components of energy for unstable case
7. Trajectory connects two saddle points
8. Illustration for Theorem 5.2
9. Fault on line 3-5 at 0.04 sec., cleared at 0.36sec.
10. Fault on line 3-5 at 0.04 sec., cleared at 0.36 sec.
11. Fault on line 3-5 at 0.04 sec., cleared at 0.38 sec.
12. Generator angles for sustained fault on line 3-5.
13. Energy functions for sustained fault on line 3-5.
14. Critical clearing time for fault on line 1-6 is 0.34 sec.
15. Generator angles for sustained fault on line 1-6.
16. Energy functions for sustained fault on line 3-5.

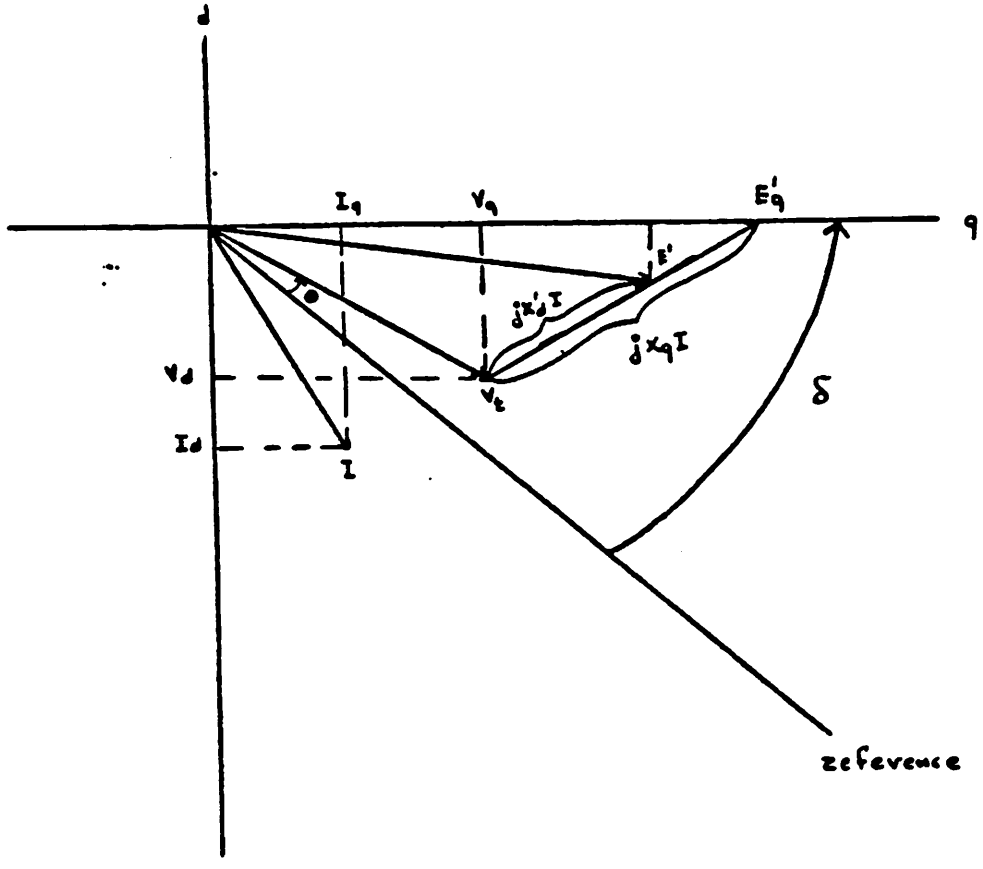


**Figure 1.**

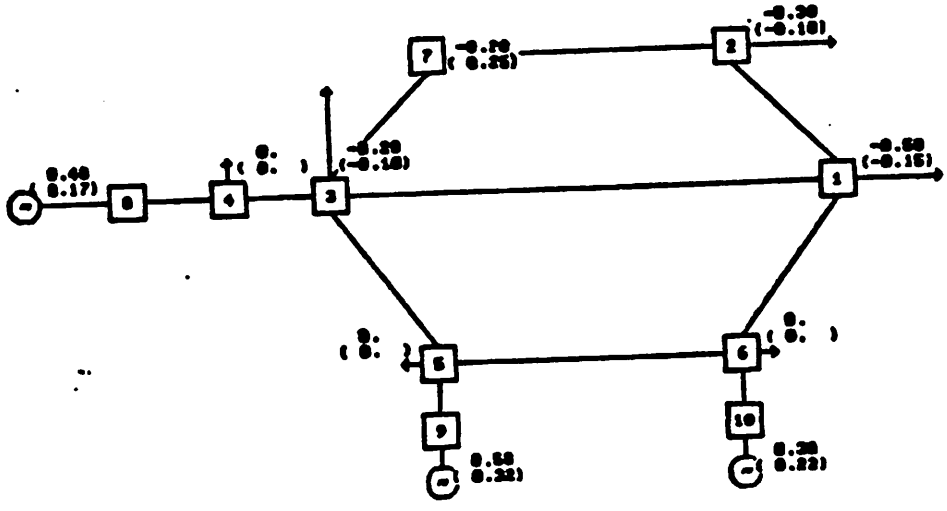

**Figure 2.**

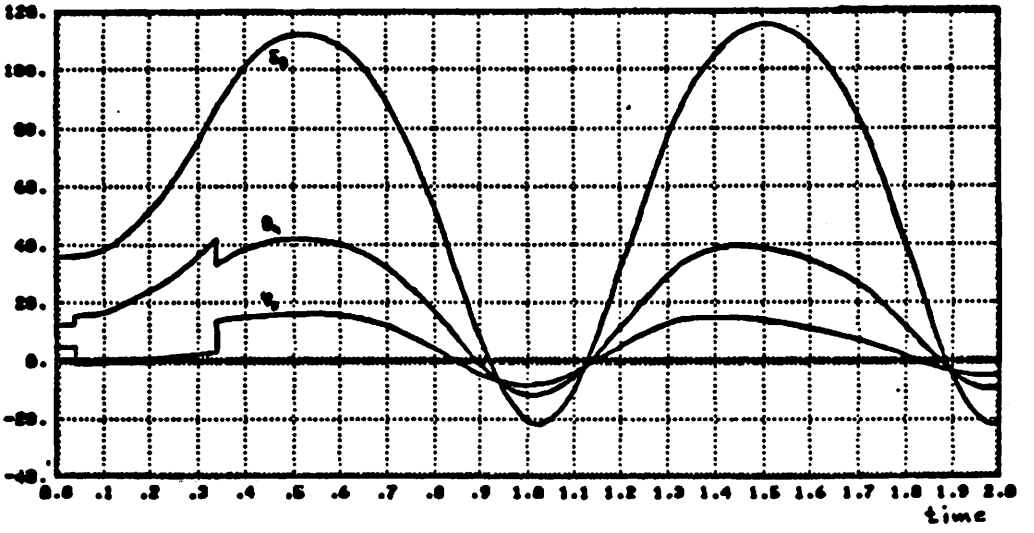


Figure 3

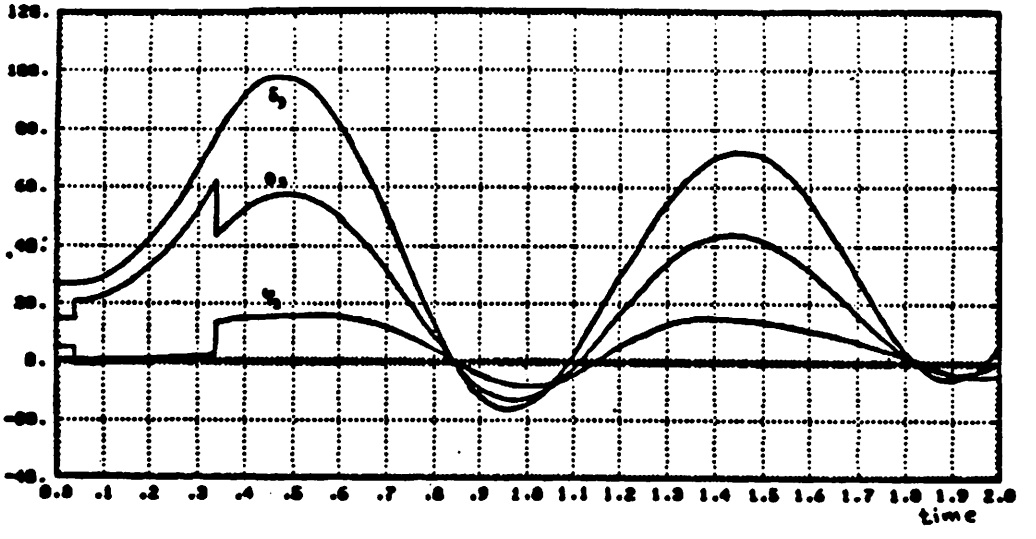


Figure 4

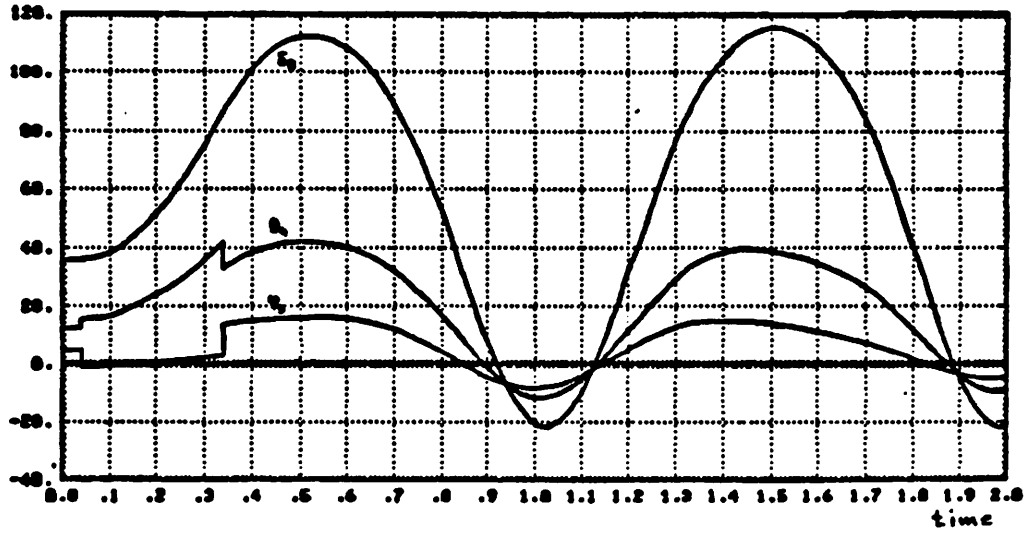


**Figure 3**

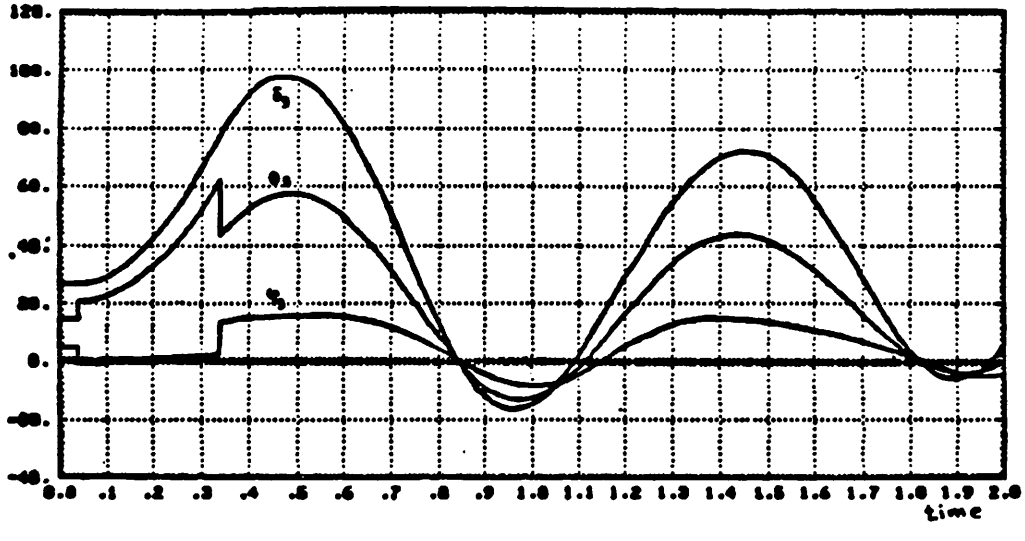


**Figure 4**

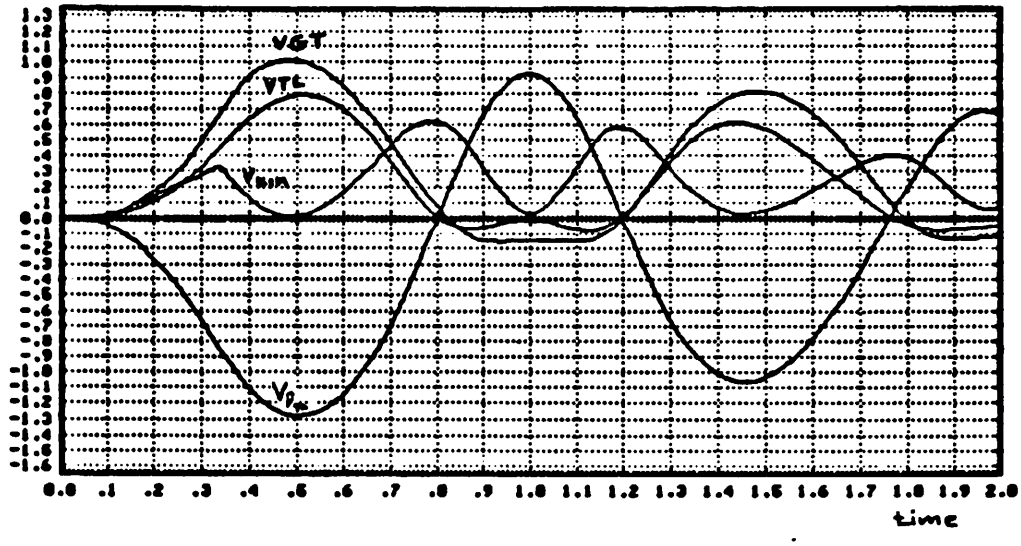


**Figure 5**

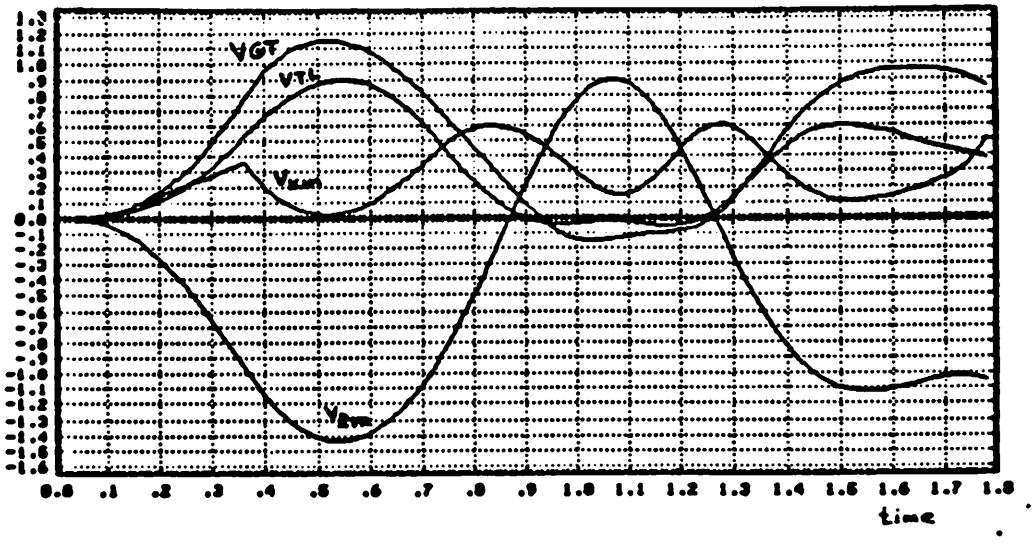


**Figure 6**

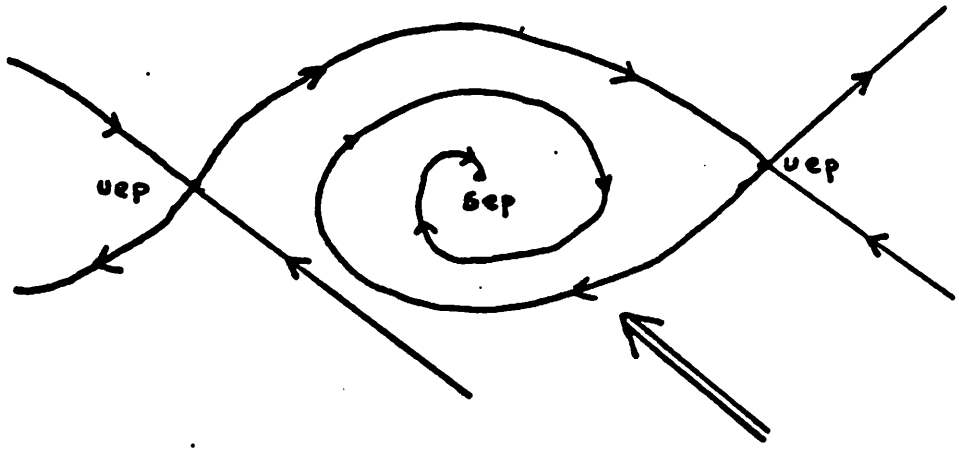


Figure 7

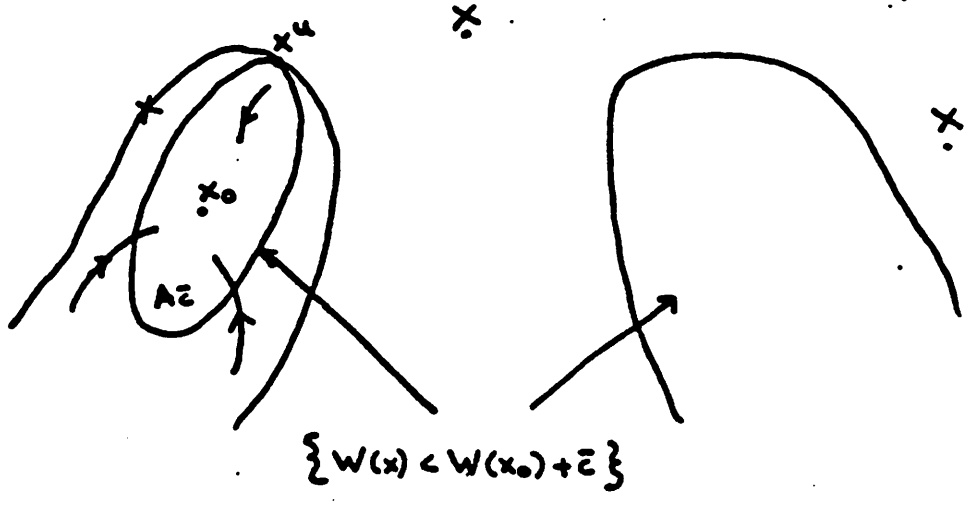


Figure 8

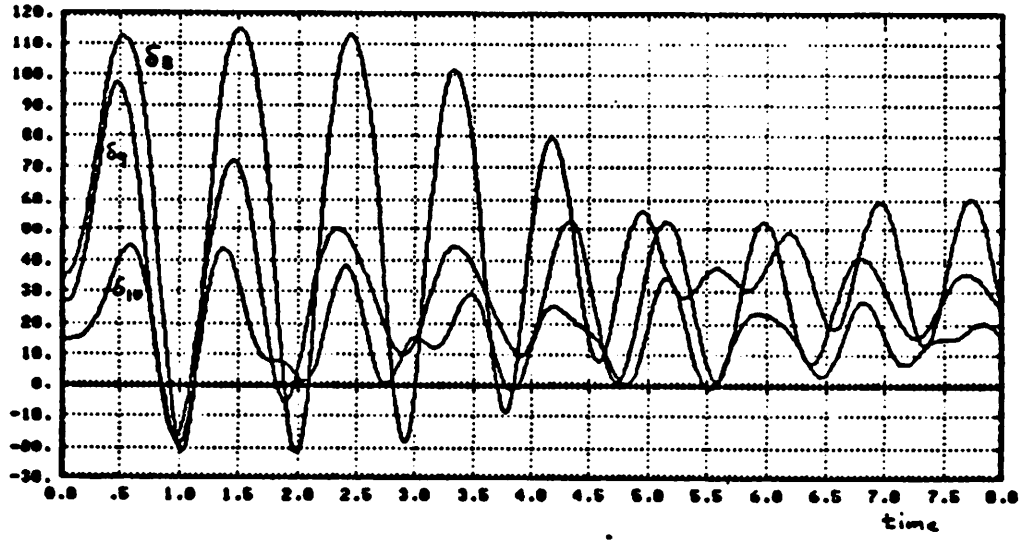


**Figure 9**

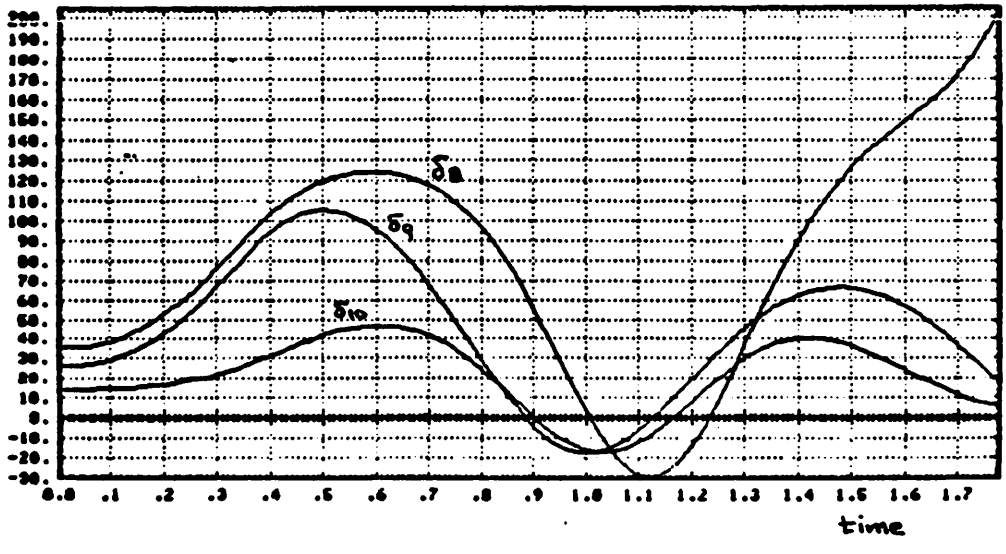


**Figure 10**

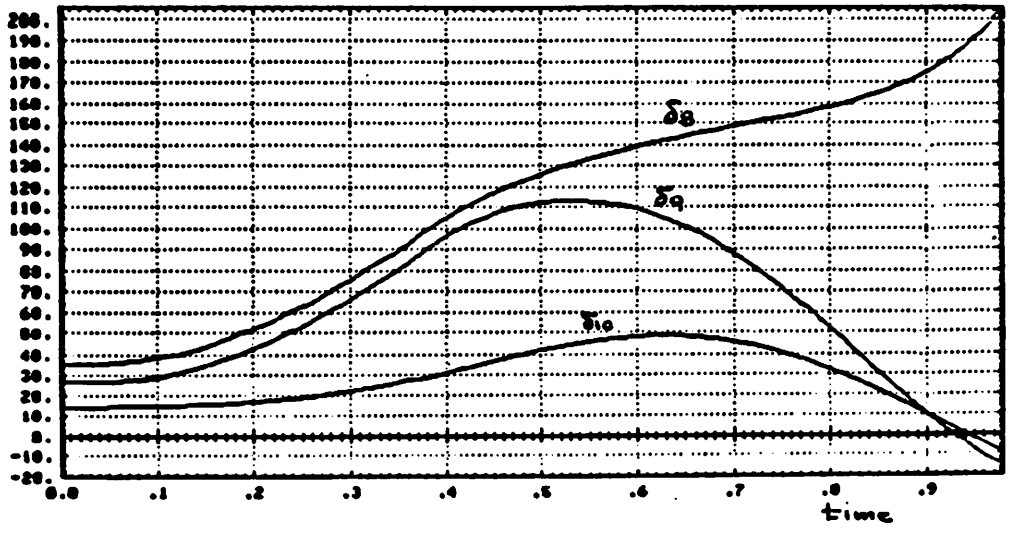


**Figure 11**

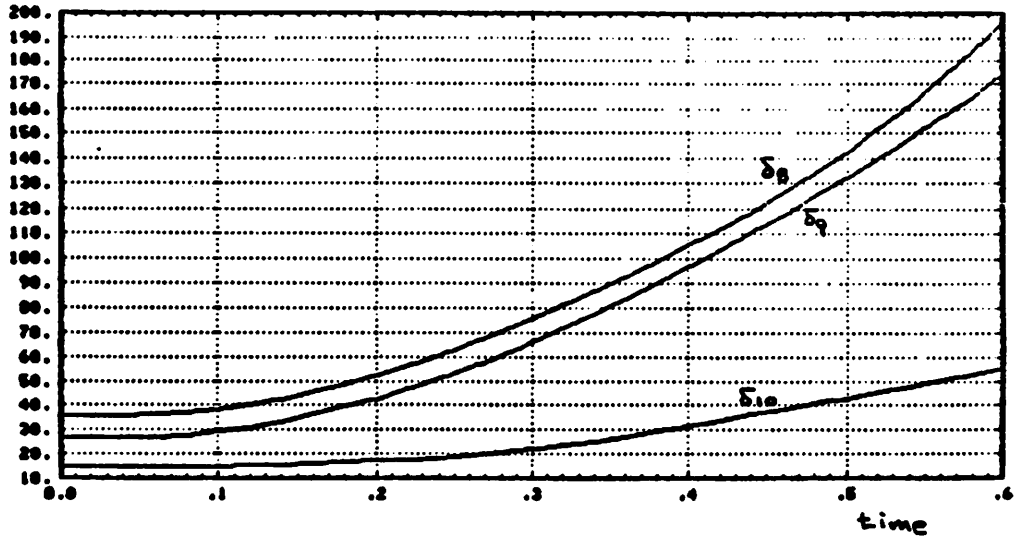


**Figure 12**

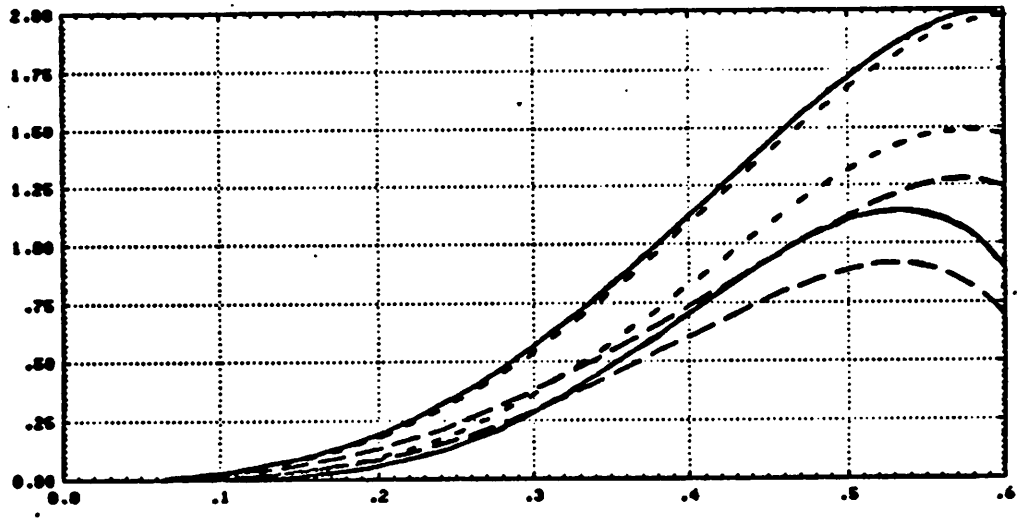


**Figure 13 : Energy Functions**

——— : Whole System

— — : Generator 8

— — — : Generator 9

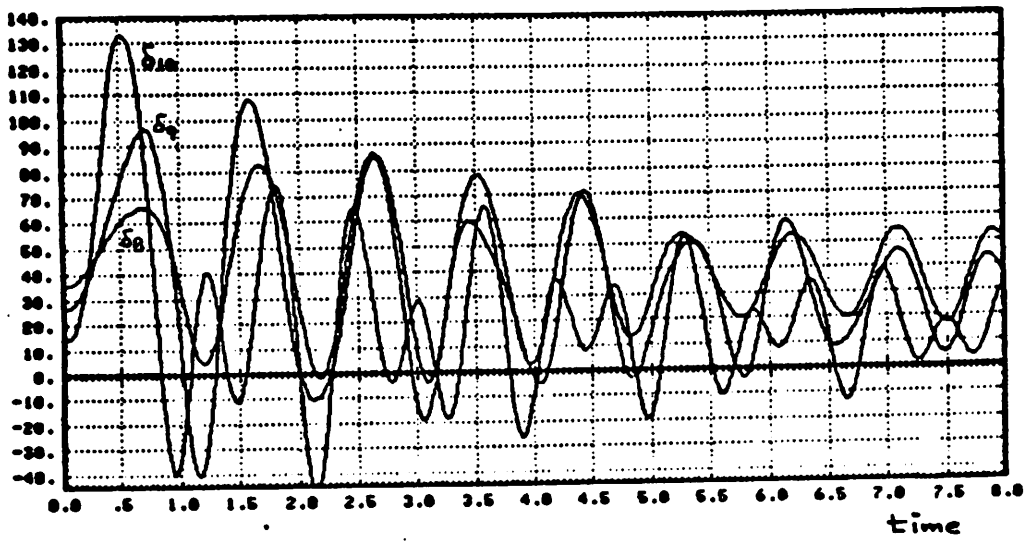


**Figure 14**

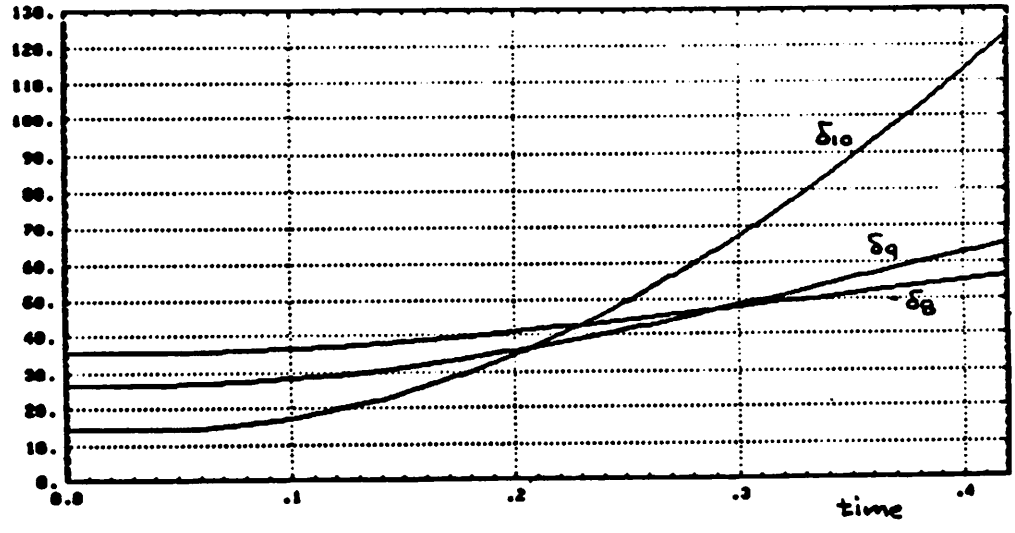


**Figure 15**

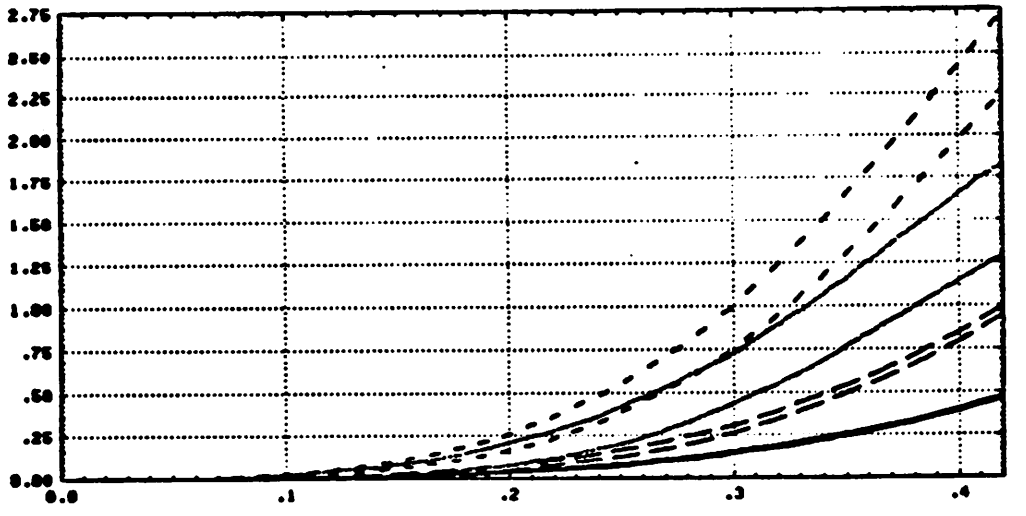


**Figure 16 : Energy Functions**

**·····: Whole System**

**———: Generator 8**

**— —: Generator 9**

**– – –: Generator 10**